Inorg. Chem. **2007**, *46*, 6647–6660

Construction of $[(\eta^5\text{-}C_5Me_5)MoS_3Cu_3]$-Based Supramolecular Assemblies from the $[(\eta^5\text{-}C_5Me_5)MoS_3(CuNCS)_3]^-$ Cluster Anion and Multitopic Ligands with Different Symmetries

Wen-Hua Zhang,[†,‡] Ying-Lin Song,[§] Zhi-Gang Ren,[†] Hong-Xi Li,[†] Ling-Ling Li,[†] Yong Zhang,[†] and Jian-Ping Lang*[,†,‡]

Key Laboratory of Organic Synthesis of Jiangsu Province, School of Chemistry and Chemical Engineering, Suzhou University, Suzhou 215123, Jiangsu, P. R. China, State Key Laboratory of Organometallic Chemistry, Shanghai Institute of Organic Chemistry, Chinese Academy of Sciences, Shanghai 200032, P. R. China, and School of Physical Science and Technology, Suzhou University, Suzhou 215006, Jiangsu, P. R. China

Received April 22, 2007

The assembly of a new family of $[(\eta^5\text{-}C_5Me_5)MoS_3Cu_3]$-supported supramolecular compounds from a preformed cluster $[PPh_4][(\eta^5\text{-}C_5Me_5)MoS_3(CuNCS)_3]\cdot$DMF (**1**·DMF) with four multitopic ligands with different symmetries is described. Reactions of **1** with 1,2-bis(4-pyridyl)ethane (bpe) (C_s symmetry) or 1,4-pyrazine (1,4-pyz) (D_{2h} symmetry) in aniline gave rise to two polymeric clusters $\{[\{(\eta^5\text{-}C_5Me_5)MoS_3Cu_3\}_2(NCS)_3(\mu\text{-}NCS)(bpe)_3]\cdot 3\text{aniline}\}_n$ (**2**) and $[(\eta^5\text{-}C_5Me_5)MoS_3Cu_3(1,4\text{-pyz})(\mu\text{-}NCS)_2]_n$ (**3**). On the other hand, solid-state reactions of **1** with 2,4,6-tri(4-pyridyl)-1,3,5-triazine (tpt) (D_{3h} symmetry) or 5,10,15,20-tetra(4-pyridyl)-21*H*,23*H*-porphyrin (H_2tpyp) (D_{4h} symmetry if 21*H* and 23*H* of the H_2tpyp are omitted) at 100 °C for 12 h followed by extraction with aniline yielded another two polymeric clusters $\{[(\eta^5\text{-}C_5Me_5)MoS_3Cu_3(tpt)(aniline)(NCS)_2]\cdot 0.75\text{aniline}\cdot 0.5H_2O\}_n$ (**4**) and $\{[(\eta^5\text{-}C_5Me_5)MoS_3Cu_3(NCS)(\mu\text{-}NCS)(H_2tpyp)_{0.4}(Cu\text{–}tpyp)_{0.1}]\cdot 2\text{aniline}\cdot 2.5\text{benzene}\}_n$ (**5**). These compounds were characterized by elemental analysis, IR spectra, UV–vis spectra, ^{1}H NMR, and X-ray analysis. Compound **2** consists of a 2D (6,3) network in which $[(\eta^5\text{-}C_5Me_5)MoS_3Cu_3]$ cores serve both a T-shaped three-connecting node and an angular two-connecting node to interconnect other equivalent units through single bpe bridges, double bpe bridges, and μ-NCS bridges. Compound **3** has a 3D diamondlike framework in which each $[(\eta^5\text{-}C_5Me_5)MoS_3Cu_3]$ core, acting as a tetrahedral connecting node, links four other neighboring units by 1,4-pyz bridges and μ-NCS bridges. Compound **4** contains a honeycomb 2D $(6,3)_{core}(6,3)_{tpt}$ network in which each cluster core, serving a trigonal-planar three-connecting node, links three pairs of equivalent cluster cores via three tpt lignads. Compound **5** has a rare scalelike 2D $(4,6^2)_{core}(4^2,6^2)_{ligand}$ network in which each cluster core acts as a T-shaped three-connecting node to link with other equivalent ones through μ-NCS bridges and H_2tpyp (or Cu–tpyp) ligands. The results showed that the formation of the four different multidimensional topological structures was evidently affected by the symmetry of the ligands used. In addition, the third-order nonlinear optical properties of **1**–**5** in aniline were also investigated by using *Z*-scan techniques at 532 nm.

Introduction

In the past decades, numerous supramolecular structures from the simple "molecular dumbbells"[1] to the most complicated three-dimensional (3D) structures including microcycles,[2] polyhedrons,[3] tubes,[4] helicates,[5] et al., have been produced by employing di-, tri-, tetra- or even hexatopic ligands to react with various metal ions. Many of these compounds are not only aesthetically appealing but also show fascinating physical and/or chemical properties.[6–8] Currently, several groups have been involved in the assembly of cluster-based supramolecular assemblies from the preformed clusters with various multitopic ligands.[6a,9–13] In some cases, the ligand symmetry effects seem to play significant roles in the

* To whom correspondence should be addressed. E-mail: jplang@suda.edu.cn.
† School of Chemistry and Chemical Engineering, Suzhou University.
‡ Shanghai Institute of Organic Chemistry.
§ School of Physical Science and Technology, Suzhou University.

10.1021/ic700762x CCC: $37.00
Published on Web 07/13/2007

formation of discrete cluster-supported supramolecules with specific architectures. For example, refluxing a mixture of $[Re_6(\mu_3\text{-}Se)_8(PEt_3)_5(MeCN)]^{2+}$ and 2,4,6-tri(4-pyridy)-1,3,5-triazine (tpt) (D_{3h} symmetry) or 5,10,15,20-tetra(4-pyridyl)-21*H*,23*H*-porphyrin (H_2tpyp) (D_{4h} symmetry if 21*H* and 23*H* of the H_2tpyp are omitted) in C_6H_5Cl/CH_2Cl_2 produced the C_3- or C_4-symmetrical cluster oligomeric species $\{[Re_6(\mu_3\text{-}Se)_8(PEt_3)_5]_3(tpt)\}^{6+}$ and $\{[Re_6(\mu_3\text{-}Se)_8(PEt_3)_5]_4(H_2tpyp)\}^{8+}$, respectively.[11c] The distinct symmetry of the tpt and H_2tpyp ligands is likely to be the driving force for the formation of the two highly symmetrical clusters. However, to the best of our knowledge, few examples have been reported to explore the effects of ligand symmetry on the formation of multidimensional cluster-based supramolecular arrays.[10a,11c]

On the other hand, in the past decades, the chemistry of Mo(W)/Cu/S clusters derived from thiomolybdate or thiotungstate have been extensively investigated due to their rich chemistry and their relations to biological systems, catalytic processes, and advanced materials.[14−18] We have recently been involved in the construction of Mo(W)/Cu/S cluster-based supramolecular structures.[19] However, the rational design and construction of such cluster-based structures remains a great challenge due to the limited number of suitable Mo(W)/Cu/S cluster precursors and the difficulty in the isolation of the resulting assemblies. In our previous reports, we mainly dedicated our efforts to exploring how the fixed geometry of the preformed clusters affected the formation of cluster-based structures. During this process, the effects of the ligand symmetry on the assembly of Mo(W)/Cu/S cluster-based arrays gradually drew our attention. For example, the preformed cluster $[WS_4Cu_4I_6]^{4-}$ reacted with D_{2h}-symmetrical 4,4-bipy or C_2-symmetrical dipyridylsulfide (dps) affording two totally different $[WS_4Cu_4]$-based supramolecular compounds, $\{[WS_4Cu_4(4,4\text{-bipy})_4][WS_4Cu_4I_4(4,4\text{-bipy})_2]\}_n$ (3D porous structure)[19c] and $[WS_4Cu_4I_2(dps)_3]_n$

(1) (a) Lu, M.; Wei, Y. G.; Xu, B. B.; Cheung, C. F.; Peng, Z. H.; Powell, D. R. *Angew. Chem., Int. Ed.* **2002**, *41*, 1566−1568. (b) Haino, T.; Matsumoto, Y.; Fukazawa, Y. *J. Am. Chem. Soc.* **2005**, *127*, 8936−8937. (c) Hori, A.; Sawada, T.; Yamashita, K.; Fujita, M. *Angew. Chem., Int. Ed.* **2005**, *44*, 4896−4899. (d) Chen, W. Z.; Ren, T. *Inorg. Chem.* **2006**, *45*, 9175−9177.

(2) (a) Leininger, S.; Olenyuk, B.; Stang, P. J. *Chem. Rev.* **2000**, *100*, 853−908. (b) Holliday, B. J.; Mirkin, C. A. *Angew. Chem., Int. Ed.* **2001**, *40*, 2022−2043. (c) Dinolfo, P. H.; Williams, M. E.; Stern, C. L.; Hupp, J. T. *J. Am. Chem. Soc.* **2004**, *126*, 12989−13001.

(3) (a) MacGillivray, L. R.; Atwood, J. L. *Angew. Chem., Int. Ed.* **1999**, *38*, 1018−1033. (b) Moulton, B.; Lu, J. J.; Mondal, A.; Zaworotko, M. J. *Chem. Commun.* **2001**, 863−864. (c) Fujita, M.; Tominaga, M.; Hori, A.; Therrien, B. *Acc. Chem. Res.* **2005**, *38*, 369−378.

(4) (a) Hong, M. C.; Zhao, Y. J.; Su, W. P.; Cao, R.; Fujita, M.; Zhou, Z. Y.; Chan, A. S. C. *Angew. Chem., Int. Ed.* **2000**, *39*, 2468−2470. (b) Yamaguchi, T.; Tashiro, S.; Tominaga, M.; Kawano, M.; Ozeki, T.; Fujita, M. *J. Am. Chem. Soc.* **2004**, *126*, 10818−10819.

(5) (a) Lehn, J.-M. *Supramolecular Chemistry Concepts and Perspectives*; VCH: Weinheim, Germany, 1995; p 139. (b) Piguet, C.; Bemardinelli, G.; Hopfgartner, G. *Chem. Rev.* **1997**, *97*, 2005−2062. (c) McMorran, D. A.; Steel, P. J. *Angew. Chem., Int. Ed.* **1998**, *37*, 3295−3297. (d) Albrecht, M.; Witt, K.; Röttele, H.; Fröhlich, R. *Chem. Commun.* **2001**, 1330−1131. (e) Matthews, C. J.; Onions, S. T.; Morata, G.; Davis, L. J.; Health, S. L.; Price, D. J. *Angew. Chem., Int. Ed.* **2003**, *42*, 3166−3169.

(6) (a) Eddaoudi, M.; Moler, D. B.; Li, H. L.; Chen, B. L.; Reineke, T. M.; O'Keeffe, M.; Yaghi, O. M. *Acc. Chem. Res.* **2001**, *34*, 319−330. (b) Moulton, B.; Zaworotko, M. J. *Chem. Rev.* **2001**, *101*, 1629−1658. (c) Rosi, N. L.; Eckert, J.; Eddaoudi, M.; Vadak, D. T.; Kim, J.; O'Keeffe, M.; Yaghi, O. M. *Science* **2003**, *300*, 1127−1129. (d) Chisholm, M. H.; Macintosh, A. M. *Chem. Rev.* **2005**, *105*, 2949−2976.

(7) (a) Batten, S. R.; Robson, R. *Angew. Chem., Int. Ed.* **1998**, *37*, 1460−1494. (b) Blake, A. J.; Champness, N. R.; Hubberstey, P.; Li, W. S.; Withersby, M. A.; Schröder, M. *Coord. Chem. Rev.* **1999**, *183*, 117−138. (c) Hagrman, P. J.; Hagrman, D.; Zubieta, J. *Angew. Chem., Int. Ed.* **1999**, *38*, 2638−2684.

(8) (a) Blake, A. J.; Champness, N. R.; Khlobystov, A. N.; Parsons, S.; Schröder, M. *Angew. Chem., Int. Ed.* **2000**, *39*, 2317−2320. (b) Galan-Mascaros, J. R.; Dunbar, K. R. *Angew. Chem., Int. Ed.* **2003**, *42*, 2289−2293. (c) Kesanli, B.; Lin, W. B. *Coord. Chem. Rev.* **2003**, *246*, 305−326. (d) Kitagawa, S.; Kitaura, R.; Noro, S. *Angew. Chem., Int. Ed.* **2004**, *43*, 2334−2375. (e) Huang, X. C.; Zhang, J. P.; Chen, X. M. *J. Am. Chem. Soc.* **2004**, *126*, 13218−13219. (f) Beltran, L. M. C.; Long, J. R. *Acc. Chem. Res.* **2005**, *38*, 325−334.

(9) (a) Cotton, F. A.; Lin, C.; Murillo, C. A. *Acc. Chem. Res.* **2001**, *34*, 759−771. (b) Cotton, F. A.; Dikarev, E. V.; Petrukhina, M. A.; Schmitz, M.; Stang, P. J. *Inorg. Chem.* **2002**, *41*, 2903−2908. (c) Cotton, F. A.; Donahue, J. P.; Lichtenberger, D. L.; Murillo, C. A.; Villagrán, D. *J. Am. Chem. Soc.* **2005**, *127*, 10808−10809. (d) Cotton, F. A.; Murillo, C. A.; Villagrán, D.; Yu, R. M. *J. Am. Chem. Soc.* **2006**, *128*, 3281−3290.

(10) (a) Seidel, S. R.; Stang, P. J. *Acc. Chem. Res.* **2002**, *35*, 972−983. (b) Chifotides, H.; Dunbar, K. R. *Acc. Chem. Res.* **2005**, *38*, 146−156.

(11) (a) Roland, B. K.; Carter, C.; Zheng, Z. P. *J. Am. Chem. Soc.* **2002**, *124*, 6234−6235. (b) Zheng, Z. P. *Chem. Commun.* **2001**, 2521−2529. (c) Roland, B. K.; Selby, H. D.; Carducci, M. D.; Zheng, Z. P. *J. Am. Chem. Soc.* **2002**, *124*, 3222−3223. (d) Selby, H. D.; Roland, B. K.; Zheng, Z. P. *Acc. Chem. Res.* **2003**, *36*, 933−944. (e) Roland, B. K.; Flora, W. H.; Selby, H. D.; Armstrong, N. R.; Zheng, Z. P. *J. Am. Chem. Soc.* **2006**, *128*, 6620−6625.

(12) (a) Long, J. R.; McCarty, L. S.; Holm, R. H. *J. Am. Chem. Soc.* **1996**, *118*, 4603−4616. (b) Beauvais, L. G.; Shores, M. P.; Long, J. R. *J. Am. Chem. Soc.* **2000**, *122*, 2763−2772. (c) Bennett, M. V.; Beauvais, L. G.; Shores, M. P.; Long, J. R. *J. Am. Chem. Soc.* **2001**, *123*, 8022−8032. (d) Tulsky, E. G.; Crawford, N. R. M.; Baudron, S. A.; Batail, P.; Long, J. R. *J. Am. Chem. Soc.* **2003**, *125*, 15543−15553.

(13) (a) Jin, S.; DiSalvo, F. J. *Chem. Mater.* **2002**, *14*, 3448−3457. (b) Bain, R. L.; Shriver, D. F.; Ellis, D. E. *Inorg. Chim. Acta* **2001**, *325*, 171−174. (c) Naumov, N. G.; Cordier, S.; Perrin, C. *Angew. Chem., Int. Ed.* **2002**, *41*, 3002−3004. (d) Mironov, Y. V.; Naumov, N. G.; Brylev, K. A.; Efremova, Q. A.; Fedorov, V. E.; Hegetschweiler, K. *Angew. Chem., Int. Ed.* **2004**, *43*, 1297−1300. (e) Yan, B. B.; Zhou, H. J.; Lachgar, A. *Inorg. Chem.* **2003**, *42*, 8818−8822. (f) Yan, Z. H.; Day, C. S.; Lachgar, A. *Inorg. Chem.* **2005**, *44*, 4499−4505. (g) Wang, J. Q.; Ren, C. X.; Jin, G. X. *Chem. Commun.* **2005**, 4738−4740. (h) Wang, J. Q.; Ren, C. X.; Weng, L. H.; Jin, G. X. *Chem. Commun.* **2006**, 162−164.

(14) (a) Müller, A.; Diemann, E.; Jostes, R.; Bögge, H. *Angew. Chem., Int. Ed.* **1981**, *20*, 934−955. (b) Müller, A.; Bögge, H.; Schimanski, U.; Penk, M.; Nieradzik, K.; Dartmann, M.; Krickemeyer, E.; Schimanski, J.; Römer, C.; Römer, M.; Dornfeld, H.; Wienböker, U.; Hellmann, W. *Monatsh. Chem.* **1989**, *120*, 367−391. (c) Howard, K. E.; Rauchfuss, T. B.; Rheingold, A. L. *J. Am. Chem. Soc.* **1986**, *108*, 297−299. (d) Ansari, M. A.; Ibers, J. A. *Coord. Chem. Rev.* **1990**, *100*, 223−266. (e) Jeannin, Y.; Sécheresse, F.; Bernés, S.; Robert, F. *Inorg. Chim. Acta* **1992**, *198−200*, 493−505. (f) Wu, X. T.; Chen, P. C.; Du, S. W.; Zhu, N. Y.; Lu, J. X. *J. Cluster Sci.* **1994**, *5*, 265−285. (g) Holm, R. H. *Pure Appl. Chem.* **1995**, *67*, 217−224. (h) Hou, H. W.; Xin, X. Q.; Shi, S. *Coord. Chem. Rev.* **1996**, *153*, 25−56. (i) Wu, D. X.; Hong, M. C.; Cao, R.; Liu, H. Q. *Inorg. Chem.* **1996**, *35*, 1080−1082. (j) Coucouvanis, D. *Adv. Inorg. Chem.* **1998**, *45*, 1−73.

(15) (a) Chianelli, R. R.; Picoraro, T. A.; Halbert, T. R.; Pan, W. H.; Stiefel, E. I. *J. Catal.* **1984**, *86*, 226−230. (b) Curtis, M. D. *J. Cluster Sci.* **1996**, *7*, 247−262. (c) *Catalysis by Di- and Polynuclear Metal Cluster Complexes*; Adams, R. D., Cotton, F. A., Eds.; Wiley-VCH: New York, 1998. (d) Hernandez-Molina, R.; Sykes, A. G. *J. Chem. Soc., Dalton Trans.* **1999**, 3137−3148. (e) Hidai, M.; Kuwata, S.; Mizobe, Y. *Acc. Chem. Res.* **2000**, *33*, 46−52.

(16) (a) Holm, R. H. *Adv. Inorg. Chem.* **1992**, *38*, 1−71. (b) *Molybdenum Enzymes, Cofactors and Model Systems*; Stiefel, E. I., Coucouvanis, D., Newton, W. E., Eds.; ACS Symposium Series 535; American Chemical Society: Washington, DC, 1993. (c) *Transition Metal Sulfur Chemistry, Biological and Industrial Significance*; Stiefel, E. I., Matsumoto, K., Eds.; ACS Symposium Series 653; American Chemical Society: Washington, DC, 1996. (d) George, G. N.; Pickering, I. J.; Yu, Y. E.; Prince, R. C.; Bursakov, S. A.; Gavel, O. Y.; Moura, I.; Moura, J. J. G. *J. Am. Chem. Soc.* **2000**, *122*, 8321−8322. (e) Dobbek, H.; Gremer, L.; Kiefersauer, R.; Huber, R.; Meyer, O. *Proc. Natl. Acad. Sci. U.S.A.* **2002**, *99*, 15971−15976.

Chart 1. Structures of bpe, 1, 4-pyz, tpt, and H_2tpyp Ligands

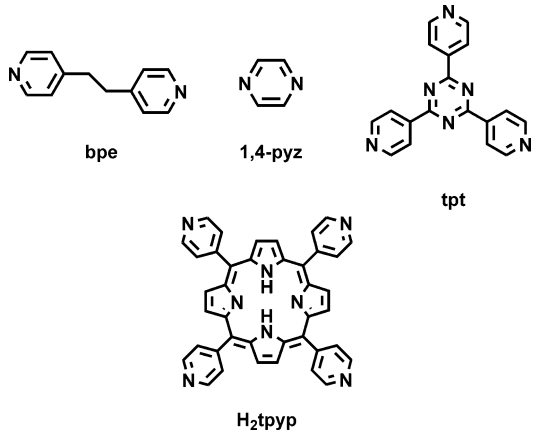

(two-dimensional (2D) layer network).[19f] In this context, we wanted to further explore these effects and thus prepared an incomplete cubane-like cluster [PPh_4][(η^5-C_5Me_5)MoS_3-($CuNCS)_3$] (**1**) as a starting material and selected four multitopic ligands with different symmetries (Chart 1): 1,2-bis(4-pyridyl)ethane (bpe) (C_s symmetry), 1,4-pyrazine (1,4-pyz) (D_{2h} symmetry), 2,4,6-tri(4-pyridy)-1,3,5-triazine (tpt) (D_{3h} symmetry), and 5,10,15,20-tetra(4-pyridyl)-21*H*,23*H*-porphyrin (H_2tpyp) (D_{4h} symmetry if 21*H* and 23*H* of the H_2tpyp are omitted).

As described later in this paper, the cluster [(η^5-C_5Me_5)-$MoS_3(CuNCS)_3]^-$ anion of **1** can be viewed as having an incomplete cubane-like [(η^5-C_5Me_5)MoS_3Cu_3] core structure in which each Cu atom has a trigonal-planar coordination geometry with a terminal thiocyanide. The three Cu centers in the cluster core of **1** may have up to six coordination sites if these thiocyanates are replaced by strong donor ligands and the coordination geometries of the Cu atoms are changed into tetrahedral ones. Under the presence of the aforementioned four ligands, the cluster core of **1** is topologically anticipated to serve as various multiconnecting nodes (nodes a−d in Scheme 1). Each node may interconnect with other nodes through the multitopic ligands to form a series of intriguing [(η^5-C_5Me_5)MoS_3Cu_3]-based supramolecular architectures (Scheme 2). With all these ideas in mind, we carried out reactions of **1** with bpe (or 1,4-pyz) in aniline or tpt (or H_2tpyp) in the solid state at low heating temperatures and isolated four unique [(η^5-C_5Me_5)MoS_3Cu_3]-based assemblies {[{(η^5-C_5Me_5)MoS_3Cu_3}$_2$($NCS)_3$(μ-NCS)(bpe)$_3$]·3aniline}$_n$ (**2**), [(η^5-C_5Me_5)MoS_3Cu_3(1,4-pyz)(μ-$NCS)_2]_n$ (**3**), {[(η^5-C_5Me_5)MoS_3Cu_3(tpt)(aniline)$(NCS)_2$]·0.75aniline·0.5H_2O}$_n$ (**4**) and {[(η^5-C_5Me_5)MoS_3Cu_3(NCS)(μ-NCS)(H_2-tpyp)$_{0.4}$(Cu−tpyp)$_{0.1}$]·2aniline·2.5benzene}$_n$ (**5**). The successful isolation of **2**−**5** may provide insights on the effect of ligand symmetries on the rational design and construction of Mo(W)/Cu/S cluster-based supramolecular compounds. Herein, we report their syntheses and crystal structures along with their third-order nonlinear optical (NLO) properties in aniline.

Experimental Section

General Procedures. [PPh_4][(η^5-C_5Me_5)MoS_3][20a] and 2,4,6-tri-(4-pyridyl)-1,3,5-triazine (tpt)[20b] were prepared according to the literature methods. Other chemicals were obtained from commercial sources and used as received. Aniline and DMF were freshly distilled under reduced pressure, while other solvents were predried over activated molecular sieves and refluxed over the appropriate drying agents under argon. The elemental analyses for C, H, and N were performed on an EA1110 CHNS elemental analyzer. The IR spectra were recorded on a Nicolet-MagNa-IR500 FT-IR spectrometer (400−4000 cm^{-1}). The UV−vis spectra were measured on a Hitachi U-2810 spectrophotometer. ^{1}H NMR spectra were recorded at ambient temperature on a Varian UNITY-400 spectrometer, and ^{1}H NMR chemical shifts were referenced to the deuterated dimethyl sulfoxide (DMSO-d_6) signal.

[PPh_4][(η^5-C_5Me_5)$MoS_3(CuNCS)_3$]·DMF (1·DMF). Compound **1**·DMF was prepared in a manner similar to that described for its tungsten analogue [PPh_4][(η^5-C_5Me_5)$WS_3(CuNCS)_3$],[17] using [PPh_4][(η^5-C_5Me_5)MoS_3] (100 mg, 0.15 mmol) and CuNCS (55 mg, 0.45 mmol) as starting materials. Yield: 143 mg (86%) based on Mo. Anal. Calcd for $C_{40}H_{42}Cu_3MoN_4OPS_6$: C, 43.49; H, 3.84; N, 5.07. Found: C, 43.64; H, 3.91; N, 5.32. IR (KBr disk): 2924 (w), 2094 (vs), 1585 (w), 1516 (w), 1483 (m), 1436 (m), 1375 (m), 1107 (s), 996 (m), 813 (w), 753 (m), 722 (s), 689 (m), 527 (s), 412 (w) cm^{-1}. ^{1}H NMR (400 MHz, DMSO-d_6): δ 7.70−7.86 (m, 20H, Ph), 2.10 (s, 15H, C_5Me_5).

{[{(η^5-C_5Me_5)MoS_3Cu_3}$_2$($NCS)_3$(μ-NCS)(bpe)$_3$]·3aniline}$_n$ (2). A dark red solution of **1** (20 mg, 0.02 mmol) in aniline (2.0 mL) was placed in a zigzag glass tube (30 cm in length, 6 mm in inner diameter) followed by the careful addition of 1.5 mL of aniline serving as a buffer band. A solution containing bpe (19 mg, 0.10 mmol) in aniline (1.5 mL) was slowly added onto the buffer band.

(17) (a) Chan, C. K.; Guo, C. X.; Wang, R. J.; Mak, T. C. W.; Che, C. M. *J. Chem. Soc., Dalton Trans*. **1995**, 753−757. (b) Zheng, H. G.; Ji, W.; Low, M. L. K.; Sakane, G.; Shibahara, T.; Xin, X. Q. *J. Chem. Soc., Dalton Trans*. **1997**, 2375−2362. (c) Shi, S. In *Optoelectronic Properties of Inorganic Compounds*; Roundhill, D. M., Fackler, J. P., Jr., Eds.; Plenum Press: New York, 1998; pp 55−105. (d) Che, C. M.; Xia, B. H.; Huang, J. S.; Chan, C. K.; Zhou, Z. Y.; Cheung, K. K. *Chem.—Eur. J*. **2001**, *7*, 3998−4006. (e) Zhang, C.; Song, Y. L.; Xu, Y.; Fun, H. K.; Fang, G. Y.; Wang, Y. X.; Xin, X. Q. *J. Chem. Soc., Dalton Trans*. **2000**, 2823−2829. (f) Coe, B. J. In *Comprehensive Coordination Chemistry II*; McCleverty, J. A., Meyer, T. J., Eds.; Elsevier Pergamon: Oxford, U.K., 2004; Vol. 9, pp 621−687.

(18) (a) Shi, S.; Ji, W.; Tang, S. H.; Lang, J. P.; Xin, X. Q. *J. Am. Chem. Soc*. **1994**, *116*, 3615−3616. (b) Lang, J. P.; Xin. X. Q. *J. Solid State Chem.* **1994**, *108*, 118−127. (c) Shi, S.; Ji, W.; Lang, J. P.; Xin, X. Q. *J. Phys. Chem*. **1994**, *98*, 3570−3572. (d) Lang, J. P.; Tatsumi, K.; Kawaguchi, H.; Lu, J. M.; Ge, P.; Ji, W.; Shi, S. *Inorg. Chem*. **1996**, *35*, 7924−7927. (e) Lang, J. P.; Kawaguchi, H.; Ohnishi, S.; Tatsumi, K. *Chem. Commun*. **1997**, 405−406. (f) Lang, J. P.; Tatsumi, K. *Inorg. Chem*. **1998**, *37*, 160−162. (g) Lang, J. P.; Tatsumi, K. *Inorg. Chem*. **1998**, *37*, 6308−6316. (h) Yu, H.; Xu, Q. F.; Sun, Z. R.; Ji, S. J.; Chen, J. X.; Liu, Q.; Lang, J. P.; Tatsumi, K. *Chem. Commun*. **2001**, 2614−2615. (i) Lang, J. P.; Ji, S. J.; Xu, Q. F.; Shen, Q.; Tatsumi, K. *Coord. Chem. Rev*. **2003**, *241*, 47−60. (j) Chen, J. X.; Xu, Q. F.; Zhang, Y.; Chen, Z. N.; Lang, J. P. *Eur. J. Inorg. Chem.* **2004**, 4247−4252. (k) Ren, Z. G.; Li, H. X.; Liu, G. F.; Zhang, W. H.; Lang, J. P.; Zhang, Y.; Song, Y. L. *Organometallics* **2006**, *25*, 4351−4357.

(19) (a) Lang, J. P.; Kawaguchi, H.; Tatsumi, K. *Chem. Commun.* **1999**, 2315−2316. (b) Lang, J. P.; Xu, Q. F.; Chen, Z. N.; Abrahams, B. F. *J. Am. Chem. Soc.* **2003**, *125*, 12682−12683. (c) Lang, J. P.; Xu, Q. F.; Yuan, R. X.; Abrahams, B. F. *Angew. Chem., Int. Ed*. **2004**, *43*, 4741−4745. (d) Lang, J. P.; Jiao, C. M.; Qiao, S. B.; Zhang, W. H.; Abrahams, B. F. *Inorg. Chem*. **2005**, *44*, 3664−3668. (e) Xu, Q. F.; Chen, J. X.; Zhang, W. H.; Ren, Z. G.; Li, H. X.; Zhang, Y.; Lang, J. P. *Inorg. Chem*. **2006**, *45*, 4055−4064. (f) Lang, J. P.; Xu, Q. F.; Zhang, W. H.; Li, H. X.; Ren, Z. G.; Chen, J. X.; Zhang, Y. *Inorg. Chem*. **2006**, *45*, 10487−10496.

(20) (a) Kawaguchi, H.; Yamada, K.; Lang, J. P.; Tatsumi, K. *J. Am. Chem. Soc.* **1997**, *119*, 10346−10358. (b) Anderson, H. L.; Anderson, S.; Sanders, J. K. M. *J. Chem. Soc., Perkin Trans. 1* **1995**, 2231−2245.

Scheme 1. Possible Topological Nodes and Frameworks Derived from **1** and Multitopic Ligands

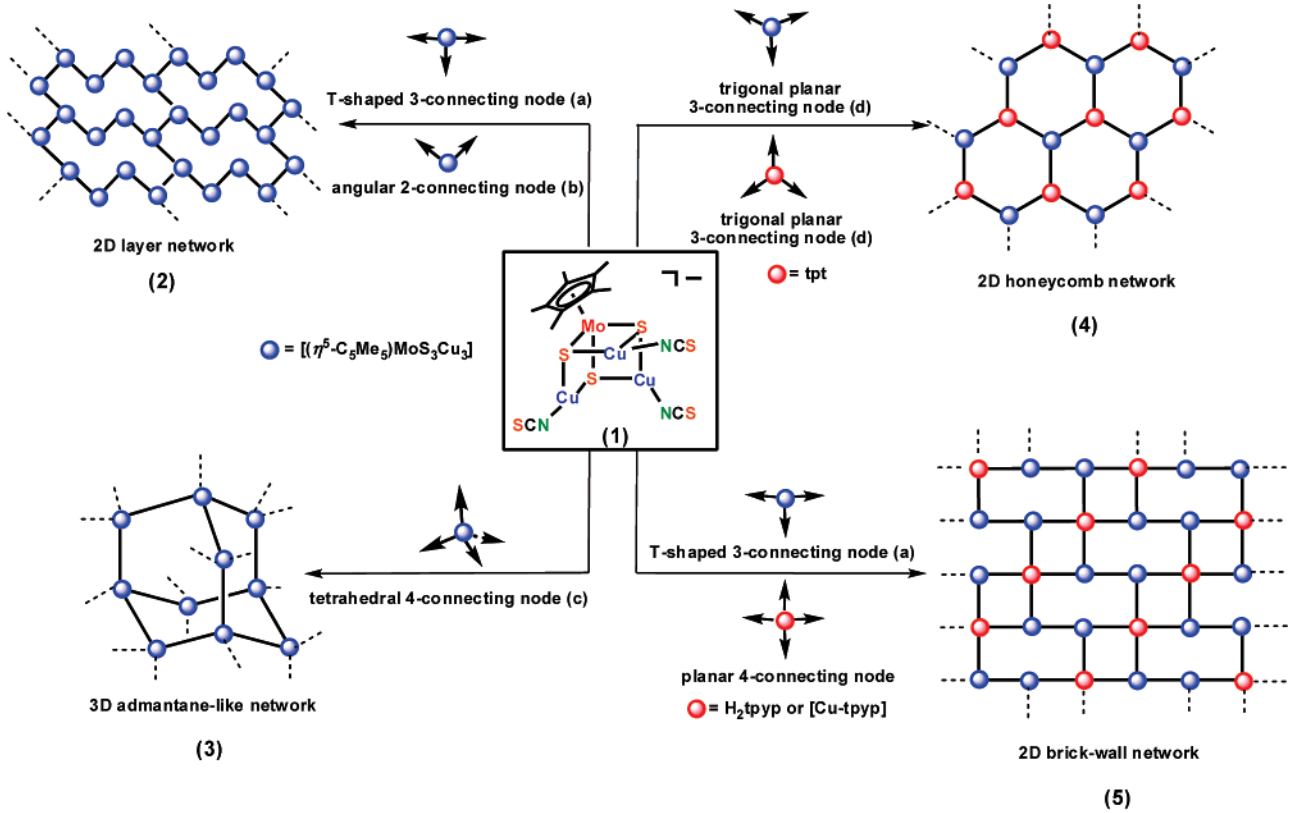

Finally, diethyl ether (3 mL) was carefully layered onto the top solution, and then the glass tube was capped with a rubber plug, which was further sealed with Parafilm. The glass tube was left to stand at room temperature for 10 days, forming black prismatic crystals of **2**, which were collected by filtration, washed with cold aniline and Et_2O (v/v = 1:5), and dried in vacuo. Yield: 15.7 mg (75%) based on Mo. Anal. Calcd for $C_{78}H_{87}Cu_6Mo_2N_{13}S_{10}$: C, 44.60; H, 4.17; N, 8.67. Found: C, 43.89; H, 4.00; N, 8.60. IR (KBr disk): 2942 (w), 2908 (w), 2115 (s), 2080 (vs), 1610 (vs), 1558 (s), 1498 (s), 1424 (s), 1384 (s), 1287 (m), 1223 (m), 1084 (m), 1022 (m), 880 (w), 826 (m), 755 (m), 694 (m), 626 (w), 549 (m), 508 (m), 415 (m) cm^{-1}. ^1H NMR (400 MHz, DMSO-d_6): δ 7.10−8.50 (m, 24H, pyridyl), 2.96 (brs, 12H, CH_2), 2.03 (s, 30H, C_5Me_5).

$[(\eta^5\text{-}C_5Me_5)MoS_3Cu_3(1,4\text{-pyz})(NCS)_2]_n$ (3). Compound **3** was prepared in a manner similar to that described for **2**, using **1** (20 mg, 0.02 mmol) and 1,4-pyz (8 mg, 0.10 mmol) as starting materials. Yield: 8 mg (55%) based on Mo. Anal. Calcd for $C_{16}H_{19}Cu_3MoN_4S_5$: C, 26.90; H, 2.68; N, 7.84. Found: C, 26.88; H, 2.30; N, 7.49. IR (KBr disk): 2940 (w), 2910 (w), 2119 (vs), 1636 (s), 1482 (m), 1420 (s), 1384 (s), 1159 (m), 1123 (m), 1084 (m), 1022 (m), 792 (m), 760 (m), 690 (m), 620 (w), 512 (m), 410 (m) cm^{-1}. ^1H NMR (400 MHz, DMSO-d_6): δ 8.82 (s, 4H, pyz), 1.99 (s, 15H, C_5Me_5).

$\{[(\eta^5\text{-}C_5Me_5)MoS_3Cu_3(tpt)(aniline)(NCS)_2]\cdot 0.75aniline\cdot 0.5H_2O\}_n$ (4). Compound **1** (20 mg, 0.02 mmol) and tpt (31 mg, 0.10 mmol) were mixed in an agate mortar and ground at ambient temperature for 30 min. The mixture was then transferred to a Pyrex glass tube (8 cm in length, 10 mm in inner diameter), which was sealed and heated in an oil bath at 100 °C for 12 h. During the reaction, the mixture gradually darkened and sintered. The resulting black solid was extracted with aniline (15 mL) to give a dark red solution and filtered. Diethyl ether (30 mL) was layered onto the filtrate to afford black block crystals of **4**, which were collected and washed with cold aniline/Et_2O (v/v = 1:5) and dries in vacuo. Yield: 10 mg (45%) based on Mo. Anal. Calcd for $C_{40.5}H_{40}Cu_3MoN_{9.75}O_{0.5}S_5$: C, 43.49; H, 3.63; N, 12.21. Found: C, 43.10; H, 3.49; N, 12.30. IR (KBr disk): 3071 (w), 3036 (w), 2120 (s), 2088 (s) 1929 (w), 1621 (vs), 1602 (vs), 1499 (vs), 1430 (m), 1385 (m), 1276 (s), 1175 (m), 1066 (w), 1027 (m), 996 (m), 881 (m), 826 (m), 753 (s), 692 (s), 623 (w), 504 (m), 412 (w) cm^{-1}. ^1H NMR (400 MHz, DMSO-d_6): δ 8.53−8.99 (m, 12H, pyridyl), 6.53−6.99 (m, 5H, Ph), 1.94 (s, 15H, C_5Me_5).

$\{[(\eta^5\text{-}C_5Me_5)MoS_3Cu_3(NCS)(\mu\text{-}NCS)(H_2tpyp)_{0.4}(Cu{-}tpyp)_{0.1}]\cdot 2aniline\cdot 2.5benzene\}_n$ (5). Compound **5** was prepared in a manner similar to that described for **4**, using **1** (20 mg, 0.02 mmol) and H_2tpyp (62 mg, 0.10 mmol) as starting materials. After extraction of the solid with aniline (15 mL) and subsequent filtration, the dark red filtrate was layered with benzene (1 mL) and Et_2O (30 mL) to produce black plates of **5**, which were collected and washed with cold aniline and Et_2O (v/v = 1:5) and dried in vacuo. Yield: 7.2 mg (25%) based on Mo. Anal. Calcd for $C_{59}H_{57}Cu_{3.1}MoN_8S_5$: C, 53.23; H, 4.30; N, 8.42. Found: C, 52.45; H, 4.22; N, 8.71. IR (KBr disk): 2940 (w), 2112 (s), 2087 (s), 1605 (vs), 1563 (m), 1497 (s), 1411 (s), 1384 (s), 1286 (m), 1222 (m), 1084 (w), 1022 (m), 970 (m), 883 (m), 800.5 (m), 752 (s), 729 (m), 694 (m), 620 (w), 510 (m), 415 (w) cm^{-1}. ^1H NMR (400 MHz, DMSO-d_6): δ 9.07 (d, 8H, 2, 6-pyridyl), 8.92 (m, 8H, pyrrole), 8.29 (d, 8H, 3, 5-pyridyl), 1.94 (s, 15H, C_5Me_5).

X-ray Structure Determination. X-ray quality single crystals of **1**·DMF and **2**−**5** were obtained directly from the above preparations. All measurements were made on a Rigaku Mercury CCD X-ray diffractometer by using graphite-monochromated Mo Kα (λ = 0.071070 nm) radiation. Each crystal was mounted at the top of a glass fiber and cooled at 153 K in a stream of gaseous nitrogen. Cell parameters were refined by using the program *CrystalClear* (Rigaku and MSc, version 1.3, 2001) on all observed reflections. The collected data were reduced by using the program

CrystalClear, and an absorption correction (multiscan) was applied, which resulted in the transmission factors ranging from 0.724 to 0.808 for **1**·DMF, 0.578 to 0.821 for **2**, 0.404 to 0.687 for **3**, 0.493 to 0.581 for **4**, and 0.416 to 0.757 for **5**. The reflection data were also corrected for Lorentz and polarization effects.

All the structures were solved by direct methods and refined on F^2 by full-matrix least-square methods using the *SHELXTL* software package.[21] For **2**, the orientation of one thiocyanate was disordered, and the occupancy ratios were refined to 0.49/0.51 for S10/S10A and N10/N10A. The methyl groups of the η^5-C_5Me_5 ligand were found to be disordered over two positions with occupancy factors of 0.48/0.52 for C20−C24/C20A−C24A. One solvated aniline molecule was observed to be split into two positions with occupancy factors of 0.62/0.38 for N13/N13A and C73−C78/C73A−C78A. For **4**, each of the two aniline solvent molecules lies on a center of inversion. Because of partial evaporation of the solvated aniline molecules in this crystal, the site-occupation factor for one aniline molecule bearing N11, C40, C41, and C42 atoms was fixed at 0.25. For **5**, the site-occupation factor for the Cu(II) center of the partially metalated Cu porphyrin was determined by identifying reasonable temperature factors and the accompanying low *R* factor during the least-square refinements.

For **1**·DMF and **2**−**5**, all non-hydrogen atoms, except for those from the disordered η^5-C_5Me_5 group, the disordered aniline solvent in **2**, and the solvated water and aniline molecules (N11, C40, C41, and C42) in **4**, were refined anisotropically. Hydrogen atoms for nitrogen atoms of the solvated aniline molecule in **2**, solvated water molecules and nitrogen atoms of solvent aniline (N11) in **4**, and two H atoms of the two pyrrol groups in **5** were not located. Other hydrogen atoms were found from Fourier maps (coordinated or solvent aniline molecules) or placed in geometrically idealized positions (C−H = 0.98 Å, with $U_{iso}(H) = 1.5U_{eq}(C)$ for methyl groups; C−H = 0.99 Å, with $U_{iso}(H) = 1.2U_{eq}(C)$ for methylene groups; C−H = 0.95 Å, with $U_{iso}(H) = 1.2U_{eq}(C)$ for aromatic rings) and constrained to ride on their parent atoms. A summary of the key crystallographic information for **1**·DMF and **2**−**5** is tabulated in Table 1.

Third-Order NLO Measurements of 1−5. The aniline solutions of **1** (3.0×10^{-5} M), **2** (3.0×10^{-5} M), **3** (3.0×10^{-5} M), **4** (1.5×10^{-5} M), and **5** (3.0×10^{-5} M) were placed in a 2 mm quartz cuvette for the third-order NLO measurements. These five compounds were stable toward air and laser light under experimental conditions. The nonlinear absorption was investigated with a linear-polarized laser light ($\lambda = 532$ nm; pulse widths = 4.5 ns; repetition rate = 2 Hz) generated from a frequency-doubled, mode-locked, Q-switched Nd:YAG laser. The spatial profiles of the optical pulses were nearly Gaussian after passing through a spatial filter. The laser beam was focused with a 30 cm focal length focusing mirror. The radius of the beam waist was measured to be 32 μm (half-width at $1/e^2$ maximum). The incident and transmitted pulse energies were measured simultaneously by two energy detectors (Laser Precision Rjp-735), which were linked to a computer by an IEEE interface.[22] The NLO properties of the samples were manifested by moving the samples along the axis of the incident laser irradiance beam (*z* direction) with respect to the focal point and with the incident laser irradiance kept constant (*Z*-scan methods).[23] The closed-aperture curves of 0.2 mm radius were placed in front of the detector to measure the transmitted energy when the assessment of the laser beam distortion was needed. To eliminate scattering effects, a lens was mounted behind the samples to collect the scattered light.

Results and Discussion

Synthetic and Spectral Aspects. In the papers we reported previously, many cluster-based supramolecular assemblies always exhibited relatively low solubilities in common organic solvents such as MeCN, DMSO, and DMF, which resulted in their low yields and, particularly, the difficulties in their crystallization and subsequent spectral and structural characterization.[19b−d] To tackle these problems, we screened many organic solvents and finally found that aniline could be a good candidate solvent because it exhibited an excellent capability for dissolving the Mo(W)/Cu/S cluster-based supramolecular compounds. In this regard, we carried out reactions of **1** with excess bpe (or 1,4-pyz) in aniline and isolated **2** and **3** in relatively high yields (Scheme 2). However, reactions of **1** in aniline with solid tpt or H_2tpyp did not form any isolable products. Analogous reactions of **1** in aniline with a suspension of tpt (or H_2tpyp) in CH_2Cl_2 at ambient temperature for 3 days also did not produce the expected Mo/Cu/S/tpt (or H_2tpyp) supramolecular compounds. Instead, a tetranuclear Mo/Cu/S cubane-like cluster $[PPh_4]_2[(\eta^5\text{-}C_5Me_5)MoS_3(CuNCS)_3Cl]$ was always isolated in relatively high yields. According to its IR spectrum, X-ray fluorescence analysis, and single-crystal X-ray crystallography, the chlorine atom in this cluster might be derived from the CH_2Cl_2 solvent (see the Supporting Information). In addition, refluxing a mixture of **1** and tpt (or H_2tpyp) in common solvents such as MeCN, DMF, or DMSO did not result in any isolable cluster-based supramolecular compounds. The main reason for these failed reactions is likely to be the very low solubility of tpt and H_2tpyp in these common organic solvents. What should we do for the reactions of **1** with tpt or H_2tpyp?

On the basis of our previous experiences in the solid-state synthesis of Mo(W)/Cu(Ag)/S clusters at low-heating temperatures,[18b,18h] we carried out the two reactions in the solid state. Compound **1** and excess tpt were mixed and firmly ground in an agate mortar at ambient temperature for 0.5 h. The black solid mixture was transferred to a Pyrex tube, which was then sealed and heated at 100 °C for 12 h. After it was cooled to ambient temperature, the resulting black solid was extracted with aniline followed by the filtration and diffusion of Et_2O into the filtrate to afford black crystals of **4** in 45% yield (Scheme 2). The solvated water molecules in this compound may be due to the presence of a small amount of water absorbed by aniline from air during the purification of the solid-state product **4**. On the other hand, analogous solid-state reactions of **1** with H_2tpyp followed by a workup similar to that used in the isolation of

(21) Sheldrick, G. M. *SHELXS97* and *SHELXL97*, *Programs for X−ray Crystal Structure Solution*; University of Göttingen: Göttingen, Germany, 1997.

(22) (a) Sherk-Bahae, M.; Said, A. A.; Wei, T. H.; Hagan, D. J.; Van, Stryland, E. W. *IEEE J. Quantum Electron.* **1990**, *26*, 760−769. (b) Sherk-Bahae, M.; Said, A. A.; Van Stryland, E. W. *Opt. Lett.* **1989**, *14*, 955−957.

(23) (a) Brunner, H.; Grassl, R.; Wachter, J.; Nuber, B.; Ziegler, M. L. *J. Organomet. Chem.* **1990**, *393*, 119−129. (b) Shi, S.; Ji, W.; Xie, W.; Chong, T. C.; Zheng, H. C.; Lang, J. P.; Xin, X. Q. *Mater. Chem. Phys.* **1995**, *39*, 298−301. (c) Zhang, C.; Song, Y. L.; Kühn, F. E.; Xu, Y.; Xin, X. Q.; Fun, H. K.; Herrmann, W. A. *Eur. J. Inorg. Chem.* **2002**, 55−64.

Table 1. Crystallographic Data for **1**·DMF and **2**−**5**

	1·DMF	**2**	**3**
formula	$C_{40}H_{42}Cu_3MoN_4OPS_6$	$C_{78}H_{81}Cu_6Mo_2N_{13}S_{10}$	$C_{16}H_{19}Cu_3MoN_4S_5$
fw	1104.67	2094.8	714.21
cryst syst	monoclinic	triclinic	orthorhombic
space group	$P2_1/c$	$P\bar{1}$	*Pnma*
a (Å)	14.924(3)	10.6942(11)	9.3447(11)
b (Å)	31.721(6)	11.0809(11)	14.7948(18)
c (Å)	9.4866(19)	36.563(4)	16.563(2)
α (deg)		83.401(6)	
β (deg)	94.31(3)	88.734(7)	
γ (deg)		80.383(7)	
V (Å^3)	4478.2(16)	4243.6(8)	2289.9(5)
Z	4	2	4
D_{calcd} (g cm^{-3})	1.638	1.639	2.072
μ (cm^{-1})	20.31	20.55	37.51
$2\theta_{max}$ (deg)	50.6	50.6	50.6
no. of reflns collected	42 999	36 681	21 279
no. of unique reflns	8172 (R_{int} = 0.062)	12 801 (R_{int} = 0.073)	2173 (R_{int} = 0.049)
no. of observed reflns	6484 [$I > 2\sigma(I)$]	9967 [$I > 2\sigma(I)$]	2037 [$I > 2\sigma(I)$]
no. of variables	512	919	146
R^a	0.0689	0.0898	0.0397
$R_w{}^b$	0.1153	0.1866	0.0690
GOF^c	1.184	1.136	1.276
$\Delta\rho_{max}$ (e Å^{-3})	0.652	1.482	0.875
$\Delta\rho_{min}$ (e Å^{-3})	−0.715	−0.770	−0.461

	4	**5**
formula	$C_{40.50}H_{38}Cu_3MoN_{9.75}O_{0.50}S_5$	$C_{59}H_{56}Cu_{3.1}MoN_3S_5$
fw	1116.17	1330.33
cryst syst	triclinic	triclinic
space group	$P\bar{1}$	$P\bar{1}$
a (Å)	10.472(2)	14.961(3)
b (Å)	16.396(3)	15.335(3)
c (Å)	16.563(3)	16.021(3)
α (deg)	60.45(3)	99.33(3)
β (deg)	89.52(3)	116.22(3)
γ (deg)	78.05(3)	108.91(3)
V (Å^3)	2405.6(11)	2910.6(19)
Z	2	2
D_{calcd} (g/cm^3)	1.541	1.518
μ (mm^{-1})	1.821	1.552
$2\theta_{max}$ (deg)	50.6	50.6
no. of reflns collected	23 417	27 723
no. of unique reflns	8724 (R_{int} = 0.027)	10 577 (R_{int} = 0.043)
no. of observed reflns	7873 [$I > 2\sigma(I)$]	8825 [$I > 2\sigma(I)$]
no. of variables	538	636
R^a	0.0568	0.0698
$R_w{}^b$	0.1562	0.1741
GOF^c	1.200	1.115
$\Delta\rho_{max}$ (e Å^{-3})	1.242	1.190
$\Delta\rho_{min}$ (e Å^{-3})	−0.888	−0.911

^{a} $R = \sum||F_o| - |F_c|/\sum|F_o|$. ^{b} $R_w = \{\sum w(F_o^2 - F_c^2)^2/\sum w(F_o^2)^2\}^{1/2}$. ^{c} GOF = $\{\sum[w((F_o^2 - F_c^2)^2)/(n - p)\}^{1/2}$, where n = number of reflections and p = total number of parameters refined.

Scheme 2. Reactions of **1** with bpe, 1,4-pyz, tpt, and H_2tpyp

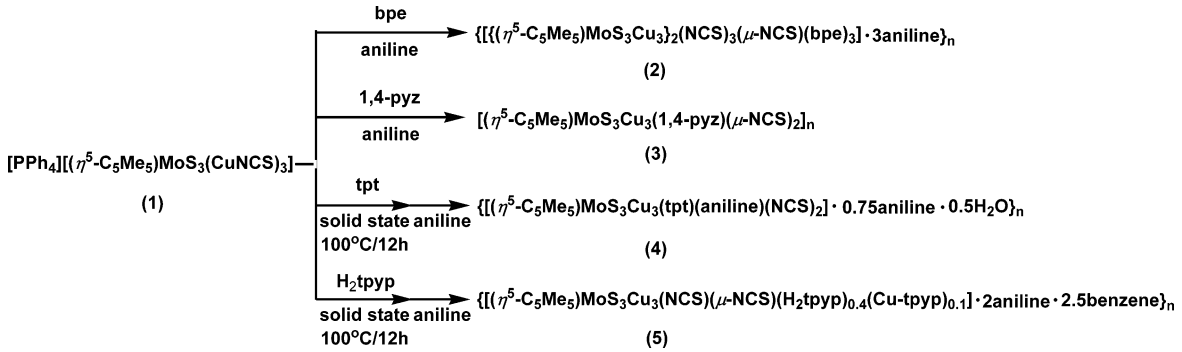

4 afforded black crystals of **5** in 25% yield (Scheme 2). Intriguingly, the free porphyrin ligand in this compound was partially metalated by Cu^{2+}. The Cu^{2+} ions may be originated from the partial decomposition of **1** during the solid-state reaction followed by the oxidation of the resulting Cu^+ ions by O_2 in air. The formation of **5** was reproduced even with

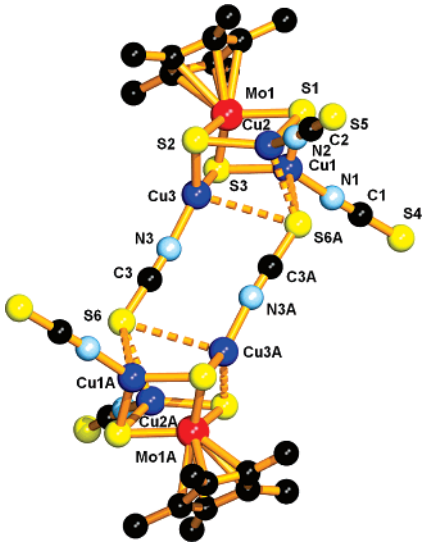

Figure 1. Perspective view of the cluster dianion of **1**. All hydrogen atoms were omitted for clarity. Symmetry code: A, $-x+1, -y+1, -z+1$.

different **1**/H_2tpyp ratios. However, **5** could not be prepared by reactions of **1** with the pure complex Cu−tpyp[24a] in 1:1 and 2:1 molar ratios. A similar phenomenon was also observed in the literature.[24b]

Solids **1**−**5** were relatively stable toward air and moisture. They were slightly soluble in DMF and DMSO but readily soluble in aniline. The elemental analyses were consistent with their chemical formula. In the IR spectra of **1**−**5**, the bands at 2093 (**1**), 2080 (**2**), 2088 (**4**), and 2087 (**5**) cm^{-1} were assigned to be the C≡N stretching vibrations of the terminal thiocyanate groups, while those at 2115 (**2**), 2119 (**3**), 2120 (**4**), and 2112 (**5**) were assumed to be those of the bridging NCS ligands. Bands at 412 (**1**), 415 (**2**), 410 (**3**), 412 (**4**), and 415 (**5**) were assigned as the bridging Mo−S stretching vibrations. The ^{1}H NMR spectra in DMSO-d_6 at room temperature showed a single resonance of η^5-C_5Me_5 at 2.10 (**1**), 2.03 (**2**), 1.99 (**3**), 1.94 (**4**), and 1.94 (**5**) ppm. In addition, other resonances in their ^{1}H NMR spectra were assigned as follows: multiplets in the 7.70−7.86 ppm region for $[PPh_4]^+$ (**1**), multiplets in the 7.10−850 ppm region for the pyridyl protons and a broad singlet at 2.96 ppm for the methylene protons of bpe (**2**), a singlet at 8.82 ppm for the 1,4-pyz liagnd (**3**), multiple resonances in the 8.53−8.99 ppm region for pyridyl groups and in the 6.53−6.99 ppm region for phenyl groups (**4**), and singlets at 9.07, 8.92, and 8.29 ppm for 2,6-pyridyl groups, pyrrole groups, and 3,5-pyridyl groups, respectively (**5**). The identities of **1**−**5** were further confirmed by X-ray crystallography.

Crystal Structure of $[PPh_4][(\eta^5\text{-}C_5Me_5)MoS_3(CuNCS)_3]\cdot$ DMF (1). Compound **1** crystallizes in the monoclinic space group $P2_1/c$, and the asymmetric unit contains half an $[(\eta^5\text{-}C_5Me_5)MoS_3(CuNCS)_3]_2^{2-}$ dianion, one $[PPh_4]^+$ cation, and one DMF solvent molecule. As shown in Figure 1, the cluster dianion is composed of two incomplete cubane-like $[(\eta^5\text{-}C_5Me_5)MoS_3(CuNCS)_3]^-$ anions, each void of which is filled with the S atom of one NCS^- from the neighboring cluster anion, forming a double cubane-like structure. There is a crystallographic inversion center located at the center of this dianion. The structure of the dianion in **1** closely resembles that of its tungsten analogue.[18e] The three Cu centers in each anion of **1** adopt an approximately trigonal-planar geometry. The mean Mo···Cu contact length (2.6453(11) Å) (Table 2) is comparable to that of $[PPh_4]_2[(\eta^5\text{-}C_5Me_5)MoS_3(CuBr)_3]_2$ (2.652(2) Å).[25] The mean Cu-μ_3-S and Mo-μ_3-S bond lengths are normal relative to those of the corresponding ones in $[PPh_4]_2[(\eta^5\text{-}C_5Me_5)MoS_3(CuBr)_3]_2$. Although the Cu2−S6A bond length (2.617(2) Å) is significantly shorter than those of the Cu1−S6A (3.028(2) Å) and Cu3−S6A (3.370(2) Å) bonds, it is longer than those of the Cu(I) complexes containing bridging thiocyanates $[Cu(\mu\text{-}NCS)(L)_2]_n$ (2.349(2) Å for L = 2-methylpyridine; 2.290(4) Å for L = quinoline).[26] Their mean value (3.005(2) Å) is comparable to that of its tungsten analogue, implying that the Cu-$(NCS)_2$Cu linkage within the dianion of **1** is weak. Therefore, in the presence of polar solvents like MeCN, DMF, and aniline, this cluster may be readily cleaved into two incomplete cubane-like $[(\eta^5\text{-}C_5Me_5)MoS_3(CuNCS)_3]^-$ anions, which could be used as a good precursor for the construction of the $[(\eta^5\text{-}C_5Me_5)MoS_3Cu_3]$-based supramolecular arrays.

Table 2. Selected Bond Distances (Å) and Angles (deg) for **1**

Mo(1)···Cu(1)	2.6370(13)	Mo(1)···Cu(2)	2.6740(11)
Mo(1)···Cu(3)	2.6249(10)	Mo(1)−S(1)	2.2886(17)
Mo(1)−S(2)	2.2868(17)	Mo(1)−S(3)	2.2917(17)
Cu(1)−N(1)	1.868(6)	Cu(1)−S(3)	2.2058(19)
Cu(1)−S(1)	2.2234(19)	Cu(2)−N(2)	1.886(6)
Cu(2)−S(2)	2.2334(19)	Cu(2)−S(1)	2.2484(18)
Cu(2)−S(6A)	2.617(2)	Cu(3)−N(3)	1.871(5)
Cu(1)−S(6A)	3.028(2)	Cu(3)−S(6A)	3.370(2)
Cu(3)−S(3)	2.2129(18)	Cu(3)−S(2)	2.2208(19)
S(6)−Cu(2A)	2.617(2)		
S(2)−Mo(1)−S(1)	105.62(6)	S(2)−Mo(1)−S(3)	105.65(6)
S(1)−Mo(1)−S(3)	105.55(7)	N(1)−Cu(1)−S(3)	123.44(19)
N(1)−Cu(1)−S(1)	122.86(19)	S(3)−Cu(1)−S(1)	110.86(7)
N(2)−Cu(2)−S(2)	120.0(2)	N(2)−Cu(2)−S(1)	117.6(2)
S(2)−Cu(2)−S(1)	108.84(7)	N(2)−Cu(2)−S(6A)	101.62(19)
S(2)−Cu(2)−S(6A)	111.53(7)	S(1)−Cu(2)−S(6A)	93.46(6)
N(3)−Cu(3)−S(3)	126.47(18)	N(3)−Cu(3)−S(2)	120.97(18)
S(3)−Cu(3)−S(2)	110.73(7)		

Crystal Structure of $\{[\{(\eta^5\text{-}C_5Me_5)MoS_3Cu_3\}_2(NCS)_3(\mu\text{-}NCS)(bpe)_3]\cdot 3aniline\}_n$ (2). Compound **2** crystallizes in the triclinic space group $P\bar{1}$, and the asymmetric unit contains half an $[\{(\eta^5\text{-}C_5Me_5)MoS_3Cu_3\}_4(NCS)_6(\mu\text{-}NCS)_2(bpe)_6]$ molecule and three aniline solvent molecules. As indicated in Figure 2, this molecule consists of two different dimeric units, $[\{(\eta^5\text{-}C_5Me_5)MoS_3Cu_3\}_2(NCS)_2(\mu\text{-}NCS)_2(bpe)_3]$ (unit 1) and $[\{(\eta^5\text{-}C_5Me_5)MoS_3Cu_3\}_2(NCS)_4(bpe)_3]$ (unit 2), which are interconnected by a single bridging bpe ligand. Unit 1 is composed of two $[(\eta^5\text{-}C_5Me_5)MoS_3Cu_3(NCS)(\mu\text{-}NCS)(bpe)]$ fragments linked by a pair of bpe ligands, and there is a crystallographic inversion center locating at the midpoint of the Mo1 and Mo1A contact (Figure 2a). Each fragment assumes the incomplete cubane-

(24) (a) Fleischer, E. B. *Inorg. Chem.* **1962**, *1*, 493−495. (b) Sharma, C. V. K.; Broker, G. A.; Huddleston, J. G.; Baldwin, J. W.; Metzger, R. M.; Rogers, R. D. *J. Am. Chem. Soc.* **1999**, *121*, 1137−1144.

(25) Lang, J. P.; Kawaguchi, H.; Ohnishi, S.; Tatsumi, K. *Inorg. Chim. Acta* **1998**, *283*, 136−144.

(26) Healy, P. C.; Pakawatchai, C.; Papasergio, R. I.; Patrick, V. A.; White, A. H. *Inorg. Chem.* **1984**, *23*, 3769−3776.

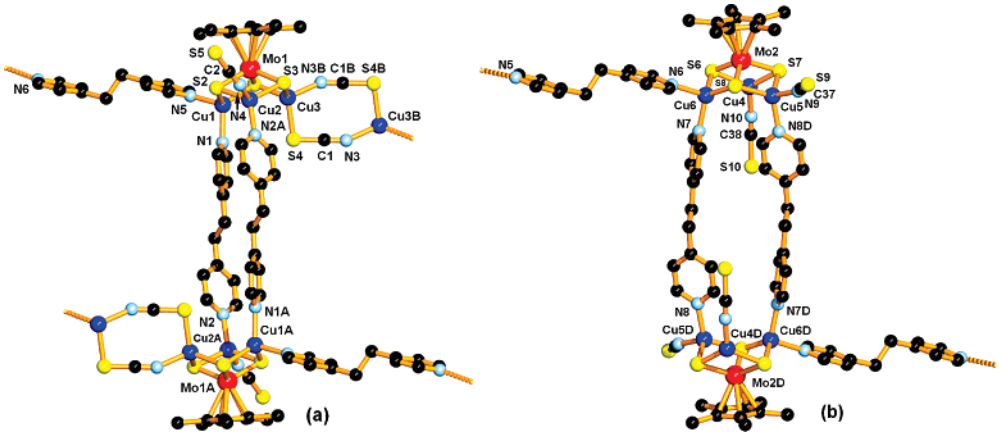

Figure 2. (a) Perspective view of the dimeric $[\{(\eta^5\text{-}C_5Me_5)MoS_3Cu_3\}_2(NCS)_2(\mu\text{-}NCS)_2(bpe)_3]$ unit (unit 1) in **2** with labeling scheme. (b) Perspective view of the dimeric $[\{(\eta^5\text{-}C_5Me_5)MoS_3Cu_3\}_2(NCS)_4(bpe)_3]$ unit (unit 2) in **2** with labeling scheme. All hydrogen atoms were omitted for clarity. Symmetry codes: A, $-x+1, -y+1, -z$; B, $-x, -y+3, -z+1$; D, $-x-1, -y+2, -z+1$.

like $[(\eta^5\text{-}C_5Me_5)MoS_3Cu_3]$ core structure of **1**. However, the three copper atoms in each fragment adopt distorted-tetrahedral coordination geometries. Being coordinated by two μ_3-S atoms from the $[(\eta^5\text{-}C_5Me_5)MoS_3]$ moiety, Cu1 is coordinated by two bridging bpe ligands, Cu2 by a terminal NCS ligand and a bridging bpe ligand, and Cu3 by a pair of μ-NCS ligands. The mean Mo1···Cu contact length (2.6935(14) Å) (Table 3) is slightly longer than those of the clusters containing tetrahedrally coordinated Cu atoms such as $\{[MoOS_3Cu_3I(dpds)_2]\cdot 0.5DMF\cdot 2(MeCN)_{0.5}\}_n$ (average length 2.6820(15) Å) and $\{[MoOS_3Cu_3(dca)(4,4'\text{-bipy})_{1.5}]\cdot DMF\cdot MeCN\}_n$ (average length 2.6782(12) Å).[19f] In the case of unit 2 (Figure 2b), two incomplete cubane-like $[(\eta^5\text{-}C_5Me_5)MoS_3Cu_3(NCS)_2(bpe)]$ fragments are linked by a couple of bridging bpe ligands, forming a centrosymmetric dimeric structure. The three Cu atoms in each fragment have different coordination geometries. Being coordinated by two μ_3-S atoms from the $[(\eta^5\text{-}C_5Me_5)MoS_3]$ moiety, Cu4 is coordinated by a terminal NCS ligand, forming a trigonal-planar coordination geometry, while Cu5 and Cu6 are coordinated by a terminal NCS ligand and a bridging bpe ligand or a couple of bridging bpe ligands, forming a distorted-tetrahedral coordination geometry. For the trigonally coordinated Cu4, the Mo2···Cu4 separation (2.6365(17) Å) is close to that of **1**, while for the tetrahedrally coordinated Cu5 and Cu6, the mean Mo2···Cu contact length (2.6900(15) Å) is quite similar to that of unit 1. Within the $Cu(NCS)_2Cu$ ring in unit 1, the Cu3−S4 (2.339(3) Å) bond length is 0.28 Å shorter than that of the shortest Cu−S(SCN) bond in **1** while the Cu3−N3B bond length (2.064(10) Å) is 0.19 Å longer than that of **1**. The mean Cu−N(bpe) length (2.045(8) Å) in **2** is longer than that observed in $\{[(\eta^5\text{-}C_5Me_5)WS_3Cu_3Cl(MeCN)(1,4\text{-pyz})](PF_6)\}_n$ (1.975(1) Å).[19a] The mean Mo-μ_3-S, Cu-μ_3-S, and terminal Cu−N(NCS) bond lengths are similar to those of the corresponding ones in **1**.

From a topological perspective, each $[(\eta^5\text{-}C_5Me_5)MoS_3Cu_3]$ core in unit 1 serves as a T-shaped three-connecting node while that in unit 2 works as an angular two-connecting node. Four angular two-connecting nodes and six T-shaped three-connecting nodes interconnect through two pairs of μ-NCS bridges, four single bpe bridges, and four pairs of double bpe bridges, forming a Z-shaped unit $[\{(\eta^5\text{-}C_5Me_5)MoS_3Cu_3\}_{10}(bpe)_{12}(NCS)_{14}(\mu\text{-}NCS)_4]$ (Figure 3). This unit has two rectangle cavities, each with an area of ca. 415 Å^2. The occurrence of an angular two-connecting node and a T-shaped three-connecting node in the same structure is unprecedented in cluster-based supramolecular chemistry. Furthermore, this *Z*-shaped unit links the equivalent units

Table 3. Selected Bond Distances (Å) and Angles (deg) for **2**

Unit 1			
Mo(1)···Cu(1)	2.6881(15)	Mo(1)···Cu(2)	2.6967(15)
Mo(1)···Cu(3)	2.6966(16)	Mo(1)−S(1)	2.285(3)
Mo(1)−S(2)	2.269(3)	Mo(1)−S(3)	2.279(3)
Cu(1)−N(1)	2.046(9)	Cu(1)−N(5)	2.083(8)
Cu(1)−S(1)	2.232(3)	Cu(1)−S(2)	2.240(3)
Cu(2)−N(2A)	2.017(8)	Cu(2)−N(4)	2.079(10)
Cu(2)−S(3)	2.237(3)	Cu(2)−S(2)	2.240(3)
Cu(3)−N(3B)	2.064(10)	Cu(3)−S(1)	2.244(3)
Cu(3)−S(3)	2.265(3)	Cu(3)−S(4)	2.339(3)
S(2)−Mo(1)−S(3)	105.34(10)	S(2)−Mo(1)−S(1)	105.41(10)
S(3)−Mo(1)−S(1)	106.09(10)	N(1)−Cu(1)−N(5)	103.0(3)
N(1)−Cu(1)−S(1)	119.5(3)	S(1)−Cu(1)−S(2)	108.18(11)
N(5)−Cu(1)−S(1)	107.9(2)	N(1)−Cu(1)−S(2)	113.5(3)
N(5)−Cu(1)−S(2)	103.3(3)	S(3)−Cu(2)−S(2)	107.69(10)
N(2A)−Cu(2)−N(4)	98.2(4)	N(2A)−Cu(2)−S(3)	113.2(3)
N(4)−Cu(2)−S(3)	114.1(3)	N(2A)−Cu(2)−S(2)	122.7(3)
N(4)−Cu(2)−S(2)	100.1(3)	S(3)−Cu(3)−S(4)	122.06(13)
N(3B)−Cu(3)−S(1)	113.7(3)	N(3B)−Cu(3)−S(3)	103.9(3)
S(1)−Cu(3)−S(3)	107.97(11)	N(3B)−Cu(3)−S(4)	101.7(3)
S(1)−Cu(3)−S(4)	107.59(12)		
Unit 2			
Mo(2)···Cu(4)	2.6365(17)	Mo(2)···Cu(5)	2.7014(15)
Mo(2)···Cu(6)	2.6785(15)	Mo(2)−S(6)	2.308(3)
Mo(2)−S(7)	2.271(3)	Mo(2)−S(8)	2.274(3)
Cu(4)−N(10)	1.95(2)	Cu(4)−S(6)	2.221(3)
Cu(4)−S(7)	2.223(3)	Cu(5)−N(8D)	2.008(9)
Cu(5)−N(9)	2.057(11)	Cu(5)−S(7)	2.229(3)
Cu(5)−S(8)	2.241(3)	Cu(6)−N(7)	2.000(9)
Cu(6)−N(6)	2.118(8)	Cu(6)−S(6)	2.231(3)
Cu(6)−S(8)	2.237(3)		
S(7)−Mo(2)−S(8)	105.06(10)	S(7)−Mo(2)−S(6)	105.48(11)
S(8)−Mo(2)−S(6)	105.40(10)	N(10)−Cu(4)−S(6)	119.4(7)
N(10)−Cu(4)−S(7)	127.9(8)	S(6)−Cu(4)−S(7)	110.18(12)
N(8D)−Cu(5)−N(9)	100.4(4)	S(7)−Cu(5)−S(8)	107.64(10)
N(8D)−Cu(5)−S(7)	110.7(3)	N(9)−Cu(5)−S(7)	113.6(3)
N(8D)−Cu(5)−S(8)	117.9(3)	N(9)−Cu(5)−S(8)	106.6(4)
N(6)−Cu(6)−S(8)	102.9(3)	N(7)−Cu(6)−S(8)	118.5(3)
S(6)−Cu(6)−S(8)	109.34(11)	N(7)−Cu(6)−N(6)	100.6(3)
N(7)−Cu(6)−S(6)	114.6(3)	N(6)−Cu(6)−S(6)	109.5(2)

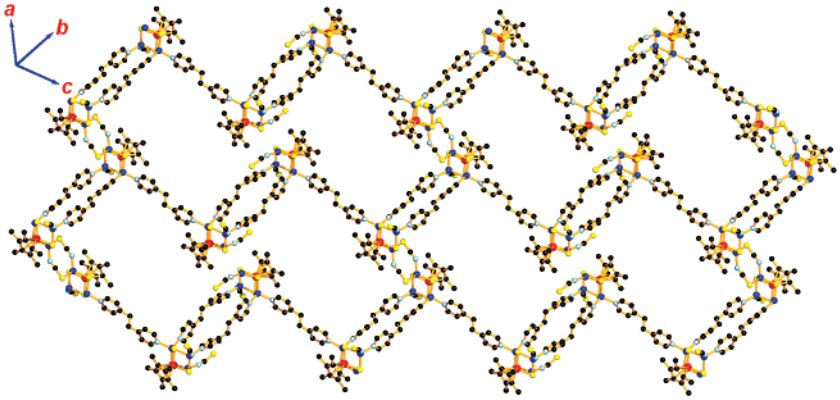

Figure 3. Extended structure of **2**, parallel to the [104] plane.

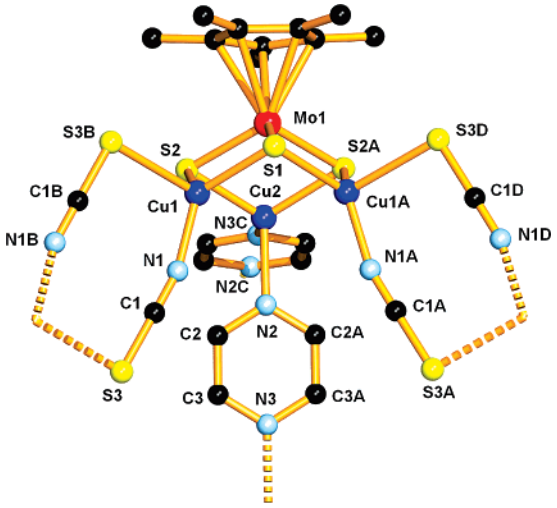

Figure 4. Perspective view of the [(η^5-C_5Me_5)MoS_3Cu_3(1,4-pyz)(μ-NCS)$_2$] molecule of **3**. All hydrogen atoms were omitted for clarity. Symmetry codes: A, x, $-y + {}^1/_2$, z; B, $-x + 2$, $-y$, $-z + 1$; C, $x - {}^1/_2$, $-y + {}^1/_2$, $-z + {}^3/_2$; D, $-x + 2$, $y + {}^1/_2$, $-z + 1$.

by a pair of single bpe bridges, a pair of double bpe bridges, and a pair of μ-NCS bridges to form a 2D (6,3) network, parallel to the [104] plane. The 2D networks are ca. 6.99 Å apart and when they are stacked along the *a* axis, and one-dimensional (1D) channels are found in the unit cell of the crystal. The channels occupy a total volume of 1010.6 Å^3 (23.8% of the total cell volume calculated by the *Platon* program[27]) and are filled with aniline solvent molecules (Supporting Information).

Crystal Structure of [(η^5-C_5Me_5)MoS_3Cu_3(1,4-pyz)(μ-NCS)$_2$]$_n$ (3). Compound **3** crystallizes in the orthorhombic space group *Pnma*, and the asymmetric unit contains half of the [(η^5-C_5Me_5)MoS_3Cu_3(1,4-pyz)(μ-NCS)$_2$] molecule. As shown in Figure 4, this molecule keeps the core structure of **1** and has a mirror plane running through the Mo, S1, Cu2, N2, N3, N2C, N3C, C6, and C9 atoms. The three Cu centers also adopt distorted-tetrahedral coordination geometries. Being coordinated by two μ_3-S atoms from the [(η^5-C_5Me_5)-MoS_3] moiety, Cu1 and Cu1A are coordinated by one N atom of one NCS ligand and one S atom from the neighboring NCS ligand, while Cu2 is coordinated by two N atoms from two bridging 1,4-pyz ligands. The mean Mo1···Cu contact (2.6785(7) Å) (Table 4) is slightly shorter than that of the corresponding ones of **2**. The mean Mo-μ_3-S and Cu-μ_3-S lengths are similar to those of the corresponding ones in **2**. Within the Cu(NCS)$_2$Cu ring, the Cu1−S3B bond length (2.5905(13) Å) is longer than that of **2**, while the Cu1−N1 bond length (1.932(4) Å) is shorter than that of **2**. In the Cu(1,4-pyz)Cu linkage, the two Cu−N bond distances are virtually the same, and their mean value (2.065(6) Å) is close to that of **2**.

Table 4. Selected Bond Distances (Å) and Angles (deg) for **3**

Mo(1)···Cu(1)	2.6933(7)	Mo(1)···Cu(1A)	2.6933(7)
Mo(1)···Cu(2)	2.6490(9)	Mo(1)−S(1)	2.2849(16)
Mo(1)−S(2)	2.2817(11)	Mo(1)−S(2A)	2.2817(11)
Cu(1)−N(1)	1.932(4)	Cu(1)−S(1)	2.2419(11)
Cu(1)−S(2)	2.2440(12)	Cu(1)−S(3B)	2.5905(13)
Cu(2)−N(3C)	2.050(6)	Cu(2)−N(2)	2.080(5)
Cu(2)−S(2)	2.2209(12)	Cu(2)−S(2A)	2.2209(12)
S(1)−Cu(1A)	2.2419(11)	S(3)−Cu(1B)	2.5905(13)
S(2)−Mo(1)−S(2A)	105.44(6)	S(2)−Mo(1)−S(1)	105.57(4)
S(2A)−Mo(1)−S(1)	105.57(4)	N(1)−Cu(1)−S(1)	123.27(13)
N(1)−Cu(1)−S(2)	116.83(12)	S(1)−Cu(1)−S(2)	108.33(5)
N(1)−Cu(1)−S(3B)	97.55(12)	S(1)−Cu(1)−S(3B)	103.34(5)
S(2)−Cu(1)−S(3B)	103.82(5)	N(3C)−Cu(2)−N(2)	91.5(2)
N(3C)−Cu(2)−S(2)	111.74(8)	N(2)−Cu(2)−S(2)	115.54(7)
N(3C)−Cu(2)−S(2A)	111.74(8)	N(2)−Cu(2)−S(2A)	115.54(7)
S(2)−Cu(2)−S(2A)	109.67(6)		

Topologically, each [(η^5-C_5Me_5)MoS_3Cu_3] cluster core works as a tetrahedral four-connecting node and is coordinated by two pairs of bridging thiocyanate groups and a pair of bridging 1,4-pyz ligands (Figure 5), which link four crystallographically equivalent cluster cores that lie at the corners of a very distorted tetrahedron, forming a single adamantine-type unit (Figure 6). This unit is further interconnected via bridging thiocyanate and 1,4-pyz ligands to form a noninterpenetrating 3D network (see the Supporting Information).

Crystal Structure of {[(η^5-C_5Me_5)MoS_3Cu_3(tpt)(aniline)-(NCS)$_2$]·0.75aniline·0.5H_2O}$_n$ (4). Compound **4** crystallizes in the triclinic space group $P\bar{1}$, and the asymmetric unit contains one discrete [(η^5-C_5Me_5)MoS_3Cu_3(tpt)(aniline)-(NCS)$_2$] molecule, one-half and one-quarter of an aniline solvent molecule, and half of a water molecule. As shown in Figure 7, this molecule again retains the core structure of **1**. Each Cu center adopts a tetrahedral coordination geometry, coordinated by two μ_3-S atoms from the [(η^5-C_5Me_5)MoS_3] moiety, one N atom from the tpt ligand, and one S atom from the terminal NCS^- (Cu1) or one N atom from an aniline

(27) Spek, A. L. *J. Appl. Crystallogr.* **2003**, *36*, 7−13.

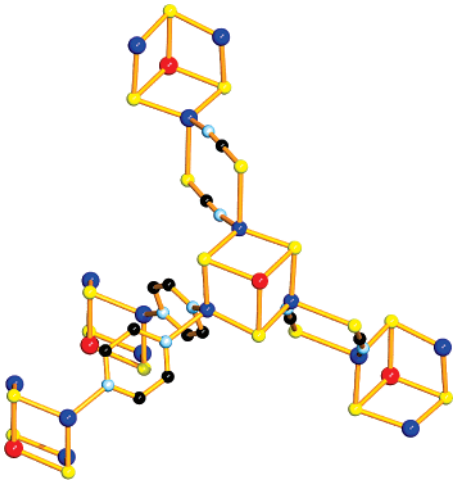

Figure 5. Perspective view of the interactions of a $[(\eta^5\text{-}C_5Me_5)MoS_3Cu_3]$ core via a pair of NCS bridges and a pair of 1,4-pyz bridges in **3**. The $(\eta^5\text{-}C_5Me_5)$ moieties were omitted for clarity.

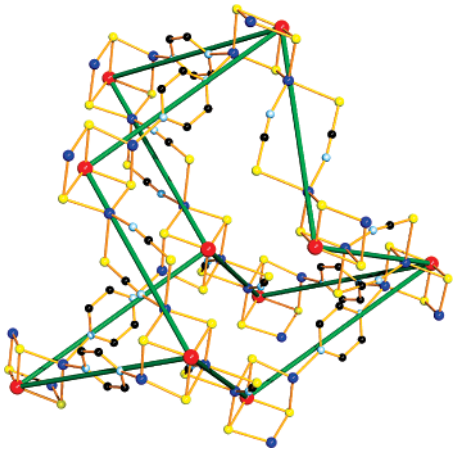

Figure 6. View of a very distorted adamantane-shaped unit within the network of **3**. The $(\eta^5\text{-}C_5Me_5)$ moieties and hydrogen atoms are omitted for clarity.

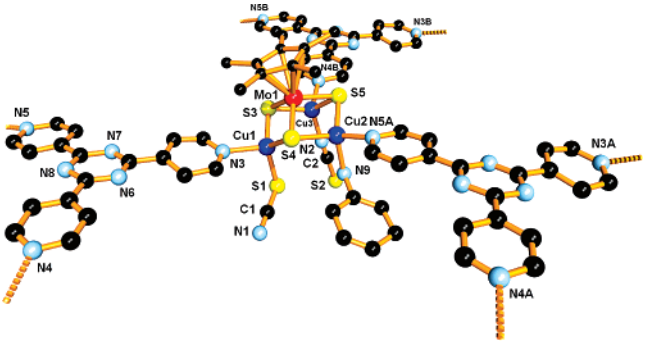

Figure 7. Perspective view of the $[(\eta^5\text{-}C_5Me_5)MoS_3Cu_3(tpt)(aniline)(NCS)_2]$ molecule of **4**. All hydrogen atoms were omitted for clarity. Symmetry codes: A, $x, y, z-1$; B, $x, y+1, z-1$.

molecule (Cu2) or one N atom from the terminal NCS^- (Cu3). It is uncommon that the two terminal NCS ligands show two different coordination preferences to Cu(I) centers in the same compound. In fact, there are only a limited number of Cu(I)/NCS complexes in which the terminal NCS ligand binds to Cu(I) via the S atom.[28] In **4**, the aniline molecules served not only as a solvent but also as a ligand, coordinating at Cu2. The mean Mo···Cu contact length

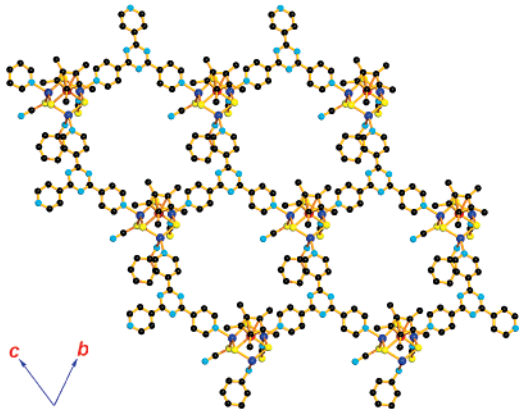

Figure 8. 2D honeycomb network of **4** looking along the *a* axis. All hydrogen atoms were omitted for clarity.

Table 5. Selected Bond Distances (Å) and Angles (deg) for **4**

Mo(1)···Cu(1)	2.6956(12)	Mo(1)···Cu(2)	2.6731(11)
Mo(1)···Cu(3)	2.6802(17)	Mo(1)−S(3)	2.2844(16)
Mo(1)−S(4)	2.2931(16)	Mo(1)−S(5)	2.2840(17)
Cu(1)−N(3)	2.110(5)	Cu(1)−S(3)	2.2421(17)
Cu(1)−S(4)	2.2669(16)	Cu(1)−S(1)	2.3152(18)
Cu(2)−N(5A)	2.060(5)	Cu(2)−N(9)	2.145(6)
Cu(2)−S(5)	2.2197(17)	Cu(2)−S(4)	2.2355(18)
Cu(3)−N(2)	1.968(6)	Cu(3)−N(4B)	2.138(5)
Cu(3)−S(3)	2.2338(17)	Cu(3)−S(5)	2.2445(17)

S(5)−Mo(1)−S(3)	105.60(6)	S(5)−Mo(1)−S(4)	105.30(6)
S(3)−Mo(1)−S(4)	106.01(6)	N(3)−Cu(1)−S(3)	105.99(14)
N(3)−Cu(1)−S(4)	103.41(13)	S(3)−Cu(1)−S(4)	108.34(6)
N(3)−Cu(1)−S(1)	105.82(14)	S(3)−Cu(1)−S(1)	113.76(7)
S(4)−Cu(1)−S(1)	118.27(6)	N(5A)−Cu(2)−N(9)	95.5(2)
N(5A)−Cu(2)−S(5)	111.39(15)	N(9)−Cu(2)−S(5)	116.20(16)
N(5A)−Cu(2)−S(4)	116.91(14)	N(9)−Cu(2)−S(4)	106.92(16)
S(5)−Cu(2)−S(4)	109.51(7)	N(2)−Cu(3)−N(4B)	100.1(2)
N(2)−Cu(3)−S(3)	116.01(17)	N(4B)−Cu(3)−S(3)	109.31(14)
N(2)−Cu(3)−S(5)	118.12(17)	N(4B)−Cu(3)−S(5)	103.11(14)
S(3)−Cu(3)−S(5)	108.69(7)		

(2.6830(12) Å) (Table 5) is in-between those of **2** and **3**. The mean Cu-μ_3-S and Mo-μ_3-S lengths are close to those in **2** and **3**.

From a topological view, the $[(\eta^5\text{-}C_5Me_5)MoS_3Cu_3]$ core of **4** is symmetrically surrounded by three tpt ligands and works as a trigonal-planar three-connecting node, which is the first example of this noted in cluster-based supramolecular chemistry. The mean deviation from the least-square plane consisting of Cu1, Cu2, Cu3, N3, N4, N5, N3A, N4A, and N5A is ca. 0.27 Å. The formation of such a topological node may be ascribed to the symmetry requirement of the rigid D_{3h}-symmetrical tpt ligand. Each tpt ligand also serves as a trigonal-planar three-connecting node and links three crystallographically equivalent $[(\eta^5\text{-}C_5Me_5)MoS_3Cu_3]$ cores. Thus, the two kinds of interconnections combine to form a honeycomb 2D $(6,3)_{core}(6,3)_{tpt}$ network extending along the *bc* plane (Figure 8). In addition, two neighboring 2D layers are tightly stacked to form a Piedfort unit[29] with a separation of 3.424 Å (Figure 9). The Piedfort units are further stacked, forming 1D channels extending along the crystallographic *b* axis. The aniline and water solvent molecules are located

(28) (a) Raper, E. S.; Clegg, W. *Inorg. Chim. Acta* **1991**, *180*, 239−244. (b) Goher, M. A. S.; Yang, Q. C.; Mak, T. C. W. *Polyhedron* **2000**, *19*, 615−621.

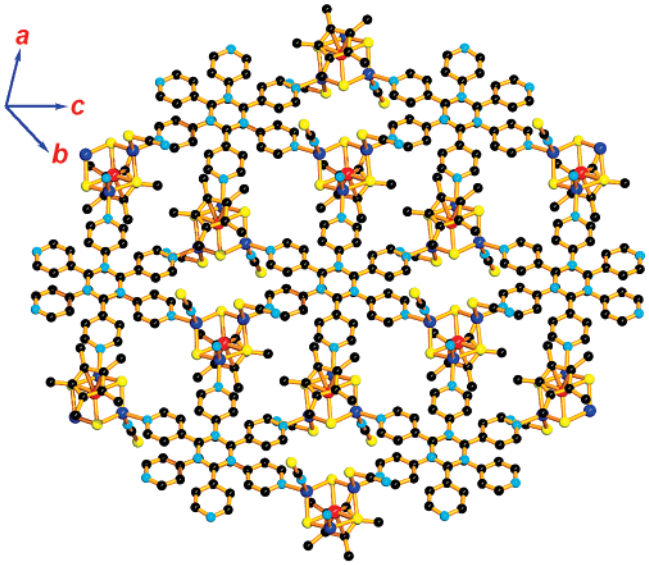

Figure 9. View of the 2D sheet pair of **4** in a staggered disposition.

in the channels or squeezed between the 2D layers (Supporting Information).

Crystal Structure of {[(η⁵-C₅Me₅)MoS₃Cu₃(NCS)(μ-NCS)(H₂tpyp)₀.₄(Cu−tpyp)₀.₁]·2aniline·2.5benzene}$_n$ (5). Compound **5** crystallizes in the triclinic space group $P\bar{1}$, and each asymmetric unit contains half of the [(η⁵-C_5Me_5)MoS_3-Cu_3(NCS)(μ-NCS)(H_2tpyp)$_{0.4}$(Cu−tpyp)$_{0.1}$]$_2$ dimer, two aniline molecules, and two and one-half benzene solvent molecules. As shown in Figure 10, the centrosymmetric dimeric molecule consists of a double incomplete cubane-like structure in which two [(η⁵-C_5Me_5)MoS_3Cu_3(NCS)(μ-NCS)(H_2-tpyp)$_{0.4}$(Cu−tpyp)$_{0.1}$] fragments are bridged by a couple of μ-NCS ligands. The core structure of **1** is retained in each fragment, but the three Cu atoms adopt different coordination geometries. Cu1 and Cu2 take a tetrahedral coordination geometry, coordinated by two μ_3-S atoms from the [(η⁵-C_5-Me_5)MoS_3] moiety, one N atom from the H_2tpyp (or Cu−tpyp) moiety, and one S atom from the bridging SCN^- (Cu1) or one N atom from the terminal NCS^- (Cu2). Cu3 has an approximately trigonal-planar coordination geometry, coordinated by two μ_3-S atoms from the [(η⁵-C_5Me_5)MoS_3] moiety and one N atom from the bridging NCS^- group. For the tetrahedrally coordinated Cu1 and Cu2 atoms, the mean Mo1···Cu contact length (2.7025(11) Å) (Table 6) is longer than those of the corresponding ones of **2**−**4**. For the trigonally coordinated Cu3 atom, the Mo1···Cu3 contact length (2.6227(11) Å) isslightly shorter than those of the corresponding ones in **1** and **2**. The Cu-μ_3-S and Mo-μ-S bond lengths are normal. The Cu1−S1 bond length is slightly longer than that found in unit 1 of **2**, while the Cu1−N1A length is similar to those of the trigonally coordinated Cu−N (NCS) bonds in **1**. Cu4 lies in the center of inversion and is coordinated by four N atoms from the pyrrole groups of tpyp,

(29) (a) Jessiman, A. S.; MacNicol, D. D.; Mallinson P. R.; Vallance, I. *J. Chem. Soc., Chem. Commun.* **1990**, 1619−1620. (b) Ke, Y. X.; Collins, D. J.; Sun, D. F.; Zhou, H. C. *Inorg. Chem.* **2006**, *45*, 1897−1899. (c) Czugler, M.; Weber, E.; Párkányi, L.; Korkas, P. P.; Bombicz, P. *Chem.—Eur. J.* **2003**, *9*, 3741−3747. (d) Saha, B. K.; Nangia, A. *Cryst. Growth Des.* **2007**, *7*, 393−401.

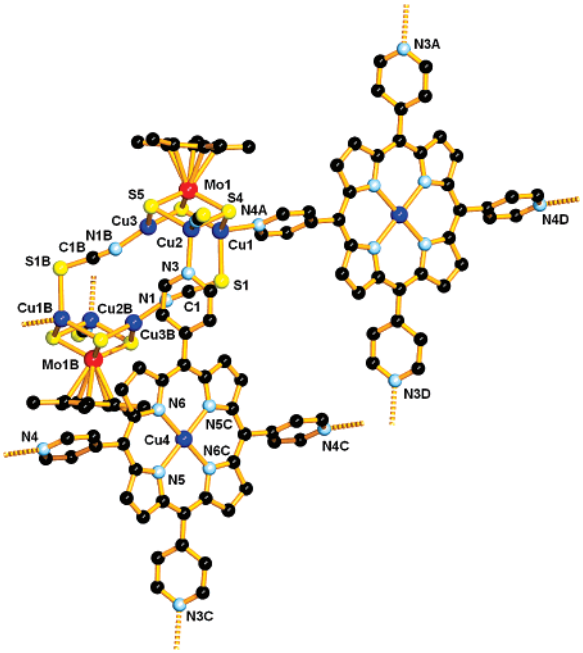

Figure 10. View of the [(η⁵-C_5Me_5)MoS_3Cu_3(NCS)(μ-NCS)(H_2tpyp)$_{0.4}$-(Cu−tpyp)$_{0.1}$]$_2$ dimer in **5** with 50% thermal ellipsoids. All hydrogen atoms were omitted for clarity. Symmetry codes: A, $x, y, z-1$; B, $-x-2, -y+1; -z+1$; C, $-x-1, -y+1, -z+2$; D, $x, y, z+1$.

Table 6. Selected Bond Distances (Å) and Angles (deg) for **5**

Mo(1)···Cu(1)	2.6849(11)	Mo(1)···Cu(2)	2.7196(19)
Mo(1)···Cu(3)	2.6227(11)	Mo(1)−S(3)	2.2993(18)
Mo(1)−S(4)	2.2732(18)	Mo(1)−S(5)	2.2848(16)
Cu(1)−N(4A)	2.084(5)	Cu(1)−S(4)	2.2439(19)
Cu(1)−S(3)	2.2449(19)	Cu(1)−S(1)	2.3494(18)
Cu(2)−N(2)	1.979(6)	Cu(2)−N(3)	2.064(5)
Cu(2)−S(5)	2.2519(19)	Cu(2)−S(4)	2.2522(16)
Cu(3)−N(1B)	1.875(6)	Cu(3)−S(3)	2.2101(17)
Cu(3)−S(5)	2.2161(19)	Cu(4)−N(5C)	2.041(5)
Cu(4)−N(5)	2.041(5)	Cu(4)−N(6)	2.056(5)
Cu(4)−N(6C)	2.056(5)		
S(4)−Mo(1)−S(5)	105.29(7)	S(4)−Mo(1)−S(3)	105.87(7)
S(5)−Mo(1)−S(3)	105.86(6)	N(4A)−Cu(1)−S(4)	105.23(15)
N(4A)−Cu(1)−S(3)	115.69(15)	S(4)−Cu(1)−S(3)	108.75(7)
N(4A)−Cu(1)−S(1)	92.83(14)	S(4)−Cu(1)−S(1)	119.05(7)
S(3)−Cu(1)−S(1)	114.35(7)	N(2)−Cu(2)−N(3)	107.6(2)
N(2)−Cu(2)−S(5)	109.16(17)	N(3)−Cu(2)−S(5)	111.50(15)
N(2)−Cu(2)−S(4)	111.40(17)	N(3)−Cu(2)−S(4)	110.09(14)
S(5)−Cu(2)−S(4)	107.10(7)	N(1B)−Cu(3)−S(3)	129.58(17)
N(1B)−Cu(3)−S(5)	117.74(17)	S(3)−Cu(3)−S(5)	111.46(7)
N(5C)−Cu(4)−N(5)	180.000(3)	N(5C)−Cu(4)−N(6)	89.27(18)
N(5)−Cu(4)−N(6)	90.73(18)	N(5C)−Cu(4)−N(6C)	90.73(18)
N(5)−Cu(4)−N(6C)	89.27(18)	N(6)−Cu(4)−N(6C)	180.000(3)

forming a square-planar coordination environment. The mean Cu−N and Mo1-μ_3-S distances are normal.

In the dimeric unit of **5**, each [(η⁵-C_5Me_5)MoS_3Cu_3] core works as a T-shaped three-connecting node to link equivalent cores through a pair of NSC bridges and two pyridyl groups of the two H_2tpyp (or Cu−tpyp) ligands (Figure 11a). In addition, each H_2tpyp (or Cu−tpyp) ligand, acing as a planar four-connecting node, links four symmetrically related Cu centers from four [(η⁵-C_5Me_5)MoS_3Cu_3] cores (Figure 11b). Interestingly, the porphyrin planes are approximately parallel to each other, while each pair of the pyridyl groups at trans positions rotate to some extent to accommodate their coordination at the copper centers. Therefore, such a

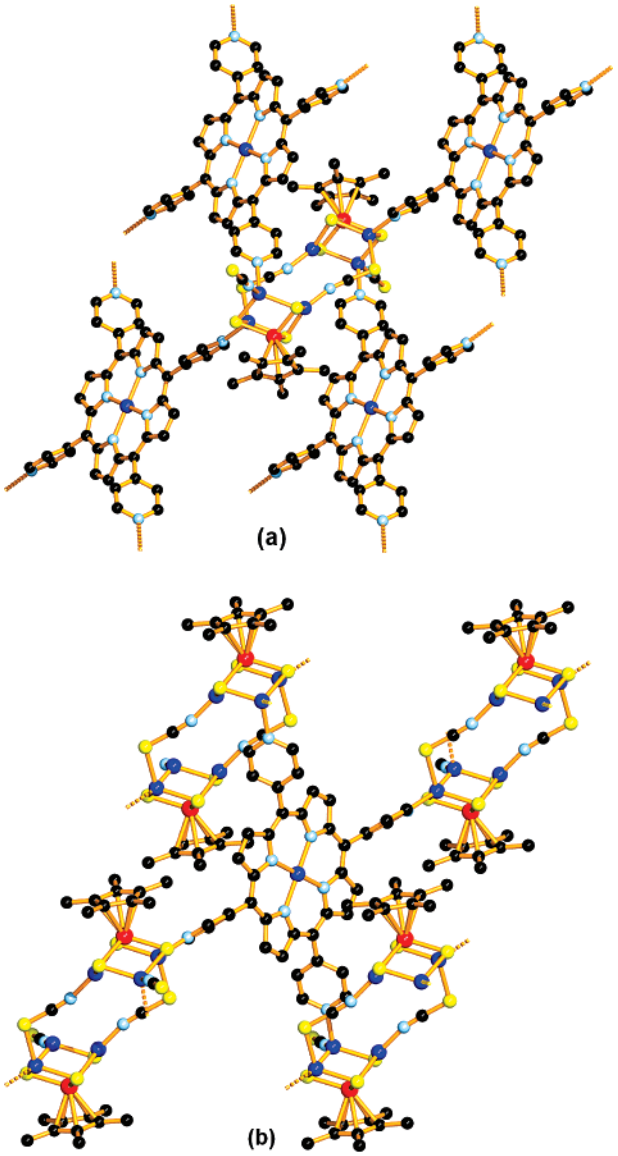

Figure 11. (a) View of the interactions of the dimer and the four H_2tpyp (or Cu−tpyp) ligands. (b) View of the interactions of one H_2tpyp (Cu−tpyp) ligand with four dimers. All hydrogen atoms were omitted for clarity.

combined interconnection between the cluster core and H_2-tpyp (or Cu−tpyp) ligands results in an unprecedented scalelike 2D $(4,6^2)_{core}(4^2,6^2)_{ligand}$ network extending along the *ac* plane (Figure 12). Alternatively, the double incomplete cubane-like $[(\eta^5\text{-}C_5Me_5)MoS_3Cu_3(NCS)(\mu\text{-}NCS)]_2$ core can be visualized as an approximate planar four-connecting node, which links with other four equivalent ones through four H_2-tpyp (or Cu−tpyp) ligands to form a 2D $(4,4)_{core}(4,4)_{ligand}$ network. The occurrence of such a topological framework is likely to indicate the presence of the four-connecting D_{4h}-symmetrical H_2tpyp (or Cu−tpyp) ligand. When these 2D layers are stacked along the *b* axis, 1D channels are again generated with a volume of 1423.9 Å^3 per unit cell (48.9% of the total cell volume). These channels are occupied by aniline and benzene solvent molecules (Supporting Information).

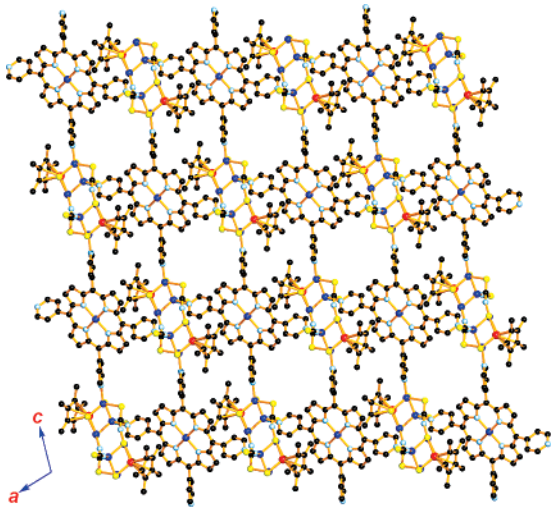

Figure 12. 2D scalelike network of **5** looking along the *b* axis. All hydrogen atoms were omitted for clarity.

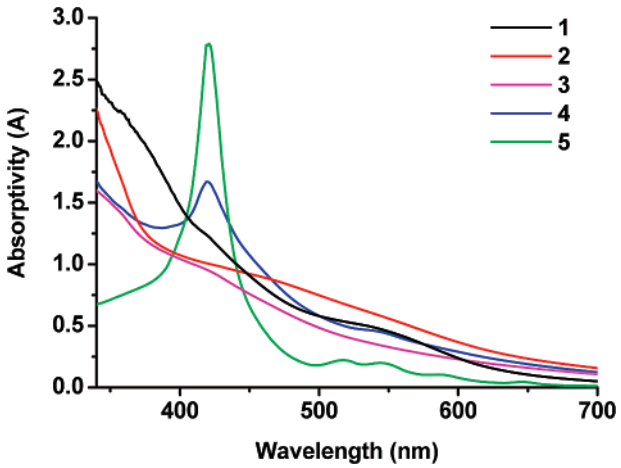

Figure 13. UV−vis curves for the aniline solutions of 3.0×10^{-5} M for **1**, 3.0×10^{-5} M for **2**, 3.0×10^{-5} M for **3**, 1.5×10^{-5} M for **4**, and 3.0×10^{-5} M for **5**.

Third-Order NLO Properties of 1−5. The UV−vis absorption spectra of **1**−**5** in aniline solution are shown in Figure 13. The electronic spectra of **1**−**3** showed similar shoulder bands at 381 nm (**1**), 421 nm (**2**), and 420 (**3**) nm. These bands are probably dominated by the S → Mo^{VI} charge-transfers in the $[(\eta^5\text{-}C_5Me_5)MoS_3]$ moieties.[30a] However, in the spectra of **4** and **5**, the similar bands may be overlapped by a strong and broad absorption at 420 nm (**4**) and 421 nm (**5**), which are tentatively assumed as the metal-to-ligand charge transfer transition[30b] (**4**) or the Soret band[30c,d] of the porphyron derivative tpyp or Cu−tpyp (**5**).

The NLO absorption performances of the aniline solutions of **1**−**5** along with pure aniline solvent were evaluated by the *Z*-scan technique under an open-aperture configuration

(30) (a) Lang, J. P.; Kawaguchi, H.; Ohnishi, S.; Tatsumi, K. *Inorg. Chim. Acta* **1998**, *283*, 136. (b) Sharma, S.; Chandra, M.; Pandey, D. S. *Eur. J. Inorg. Chem.* **2004**, 3555. (c) Konarev, D. V.; Litvinov, A. L.; Neretin, I. S.; Drichko, N. V.; Slovokhotov, Y. L.; Lyubovskaya, R. N.; Howard, J. A.; Yufit, D. S. *Cryst. Growth Des.* **2004**, *4*, 643. (d) Qi, H. R.; Zhao, H. B.; Luo, H. A.; Wang, X. Y.; Xie, Q. Y.; Peng, S. M.; Yang, P. L. *Chin. J. Anal. Chem.* **2004**, *32*, 1608.

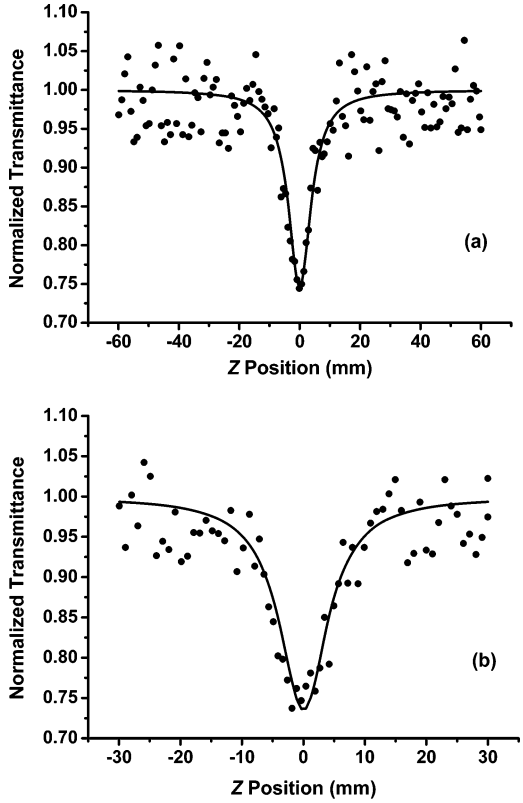

Figure 14. *Z*-Scan data for the aniline solutions of 3.0×10^{-5} M for **1** (a) and 3.0×10^{-5} M for **5** (b). The black solid spheres are experimental data, and the solid curves are the theoretical fit.

at 532 nm (Figure 14 and Supporting Information Figures S6−S8). For the pure aniline solvent, the linear transmittance for aniline was found to be very large, amounting to 97.2% (see the Supporting Information), which suggests that it has weak NLO refraction and absorption and is not enough to impact the NLO properties of complexes in aniline. Although the detailed mechanism is still unknown, the NLO absorption data obtained under the conditions used in this work can be evaluated by previous methods.[22] The nonlinear absorptive indexes α_2 for **1**−**5** were calculated to be 7.58×10^{-11} M·W^{-1} (**1**), 6.86×10^{-11} M·W^{-1} (**2**), 6.78×10^{-11} M·W^{-1} (**3**), 6.11×10^{-11} M·W^{-1} (**4**), and 7.79×10^{-11} M·W^{-1} (**5**), respectively, implying that they have good NLO absorption properties. Intriguingly, **1**−**5** were not detected to have nonlinear refractive effects, implying that their nonlinear refractive effects are weak in our experimental conditions.

In accordance with the observed α_2 values, the effective third-order susceptibilities[31] $\chi^{(3)}$ for **1**−**5** were calculated to be 2.86×10^{-12} esu (**1**), 2.78×10^{-12} esu (**2**), 2.74×10^{-12} esu (**3**), 2.47×10^{-12} esu (**4**), and 3.15×10^{-12} esu (**5**), while the corresponding hyperpolarizabilities γ values[30] were 3.09×10^{-29} esu (**1**), 2.99×10^{-29} esu (**2**), 2.96×10^{-29} esu (**3**), 2.67×10^{-29} esu (**4**), and 6.80×10^{-29} esu (**5**). These results showed that **1**−**5** possess relatively strong third-order optical nonlinearities. In addition, the third-order NLO properties for **5** were slightly better than those of **1**−**4**, which may be ascribed to the fact that **5** has relatively lower linear absorption at 532 nm than **1**−**4**.

(31) (a) Yang, L.; Dorsinville, R.; Wang, Q. Z.; Ye, P. X.; Alfano, R. R.; Zamboni, R.; Taliani. C. *Opt. Lett.* **1992**, *17*, 323−325. (b) Chen, Z. R.; Hou, H. W.; Xin, X. Q.; Yu, K. B.; Shi, S. *J. Phys. Chem.* **1995**, *99*, 8717−8721.

Conclusion

In the work reported here, we demonstrated our new efforts to explore the effects of ligand symmetry on the rational design and construction of Mo/Cu/S cluster-based supramolecular arrays. Four multitopic ligands from low symmetry (C_s) to higher symmetry (D_{4h}) were employed to react with **1** to form four unique [(η^5-C_5Me_5)MoS_3Cu_3]-based supramolecular compounds **2**−**5**. In all these compounds, the cluster core of **1** was retained and worked as multiconnecting nodes. Compound **2** shows a 2D (6,3) network in which the [(η^5-C_5Me_5)MoS_3Cu_3] cores serve both a T-shaped three-connecting node and an angular two-connecting node. Compound **3** has a 3D noninterpenetrating diamondlike framework in which each [(η^5-C_5Me_5)MoS_3Cu_3] core acts as a tetrahedral connecting node. Compound **4** has a honeycomb 2D $(6,3)_{core}$-$(6,3)_{tpt}$ network in which the [(η^5-C_5Me_5)MoS_3Cu_3] core works as a trigonal-planar three-connecting node. Compound **5** is composed of a rare scalelike 2D $(4,6^2)_{core}(4^2,6^2)_{ligand}$ network in which each [(η^5-C_5Me_5)MoS_3Cu_3] core acts as a T-shaped three-connecting node. From these results, along with our previous ones,[19] it is assumed that upon utilization of the low symmetrical bpe ligand, the [(η^5-C_5Me_5)MoS_3Cu_3] core may give rise to irregular topogical nodes, which will result in the formation of the less symmetrical structure of **2**. Meanwhile, ligands with the higher symmetries (e.g., D_{3h}-symmetrical tpt and D_{4h}-symmetrical H_2tpyp (or Cu−tpyp)) would template the [(η^5-C_5Me_5)MoS_3Cu_3] core to be the trigonal-planar three-connecting node or induce the cluster cores to dimerize to be a planar four-connecting node, which would lead to the formation of the more symmetrical structures of **4** and **5**. Although **1**−**5** exhibited good third-order NLO properties in solution, their NLO absorptive behaviors are very similar, which may be attributed to the fact that they all possess the [(η^5-C_5Me_5)MoS_3Cu_3] cluster core of **1** in their structures. For the time being, it is difficult to correlate the symmetries of the ligands used with the resulting topological structures and their NLO properties. Other factors such as the solvents used, the reaction temperatures, the shape and size of the bridging ligands, etc. may be also responsible for the composition and structure of the generated compounds. However, it is believed that ligand symmetry effects should be taken into consideration when we make more efforts toward the rational design and construction of Mo(W)/Cu/S cluster-based assemblies, especially those with better NLO properties. Studies on these respects are underway in this laboratory.

Acknowledgment. This work was supported by the National Natural Science Foundation of China (20525101), the NSF of Jiangsu Province (BK2004205), the Specialized Research Fund for the Doctoral Program of Higher Education (20050285004), the State Key Laboratory of Organometallic Chemistry of Shanghai Institute of Organic Chemistry (06-26), the Qin-Lan Project of Jiangsu Province, and the

Scientific Research Foundation for the Returned Overseas Chinese Scholars, State Education Ministry of China. We are grateful to the reviewers for their helpful suggestions.

Supporting Information Available: Crystallographic data of compounds **1**−**5** (CIF), synthesis and characterization and perspective view of $[PPh_4]_2[(\eta^5\text{-}C_5Me_5)MoS_3(CuNCS)_3Cl]$, cell-packing diagrams for **3**−**5**, and *Z*-scan data for **2**−**4** and pure aniline in PDF format. This material is available free of charge via the Internet at http://pubs.acs.org.

IC700762X